Therapeutic Potential of Vasculogenesis and Osteogenesis Promoted by Peripheral Blood CD34-positive Cells for Functional Bone Healing

Matsumoto, Tomoyuki

(Degree)
博士（医学）

(Date of Degree)
2006-09-25

(Date of Publication)
2012-08-29

(Resource Type)
doctoral thesis

(Report Number)
甲3725

(URL)
https://hdl.handle.net/20.500.14094/D1003725

Therapeutic Potential of Vasculogenesis and Osteogenesis Promoted by Peripheral Blood CD34-positive Cells for Functional Bone Healing

末梢血 CD34 陽性細胞による骨・血管再生療法の機能的骨折治癒に対する可能性

Tomoyuki Matsumoto[1,2], Atsuhiko Kawamoto[1], Ryosuke Kuroda[2], Masakazu Ishikawa[1], Yutaka Mifune[1,2], Hiroto Iwasaki[1], Masahiko Miwa[2], Miki Horii[1], Saeko Hayashi[1], Akira Oyamada[1], Hiromi Nishimura[1], Satoshi Murasawa[1], Minoru Doita[2], Masahiro Kurosaka[2], Takayuki Asahara[1, 3]

[1] Stem Cell Translational Research, Kobe Institute of Biomedical Research and Innovation / RIKEN Center for Developmental Biology

[2]Department of Orthopedic Surgery, Kobe University Graduate School of Medicine

[3] Department of Regenerative Medicine Science, Tokai University School of Medicine

---

Key words; peripheral blood CD34+ cells, vasculogenesis, osteogenesis, fracture healing

Therapeutic Potential of Vasculogenesis and Osteogenesis Promoted by Peripheral Blood CD34-positive Cells for Functional Bone Healing

Tomoyuki Matsumoto[1,2] (matsun@m4.dion.ne.jp), Atsuhiko Kawamoto[1] (kawamoto@fbri.org), Ryosuke Kuroda[2] (kurodar@med.kobe-u.ac.jp), Masakazu Ishikawa[1] (goemon@hiroshima-u.ac.jp), Yutaka Mifune[1,2] (m-ship@cdb.riken.jp), Hiroto Iwasaki[1] (hiroto@cdb.riken.jp), Masahiko Miwa[2] (masahiko@med.kobe-u.ac.jp), Miki Horii[1] (hmiki@fbri.org), Saeko Hayashi[1] (busaeko@fbri.org), Akira Oyamada[1] (a-oya@cdb.riken.jp), Hiromi Nishimura[1] (nishimura@fbri.org), Satoshi Murasawa[1] (murasawa@fbri.org), Minoru Doita[2] (doita@med.kobe-u.ac.jp), Masahiro Kurosaka[2] (kurosaka@med.kobe-u.ac.jp), Takayuki Asahara[1,3] (asa777@aol.com)

[1] Stem Cell Translational Research, Kobe Institute of Biomedical Research and Innovation / RIKEN Center for Developmental Biology

[2]Department of Orthopedic Surgery, Kobe University Graduate School of Medicine

[3] Department of Regenerative Medicine Science, Tokai University School of Medicine

Running title: Circulating CD34+ cells for fracture healing

Number of Text Pages: 38 pages

Number of Tables and Figures: 0 Tables and 6 Figures

Please address all correspondence to:

Takayuki Asahara, MD.

Stem Cell Translational Research, Kobe Institute of Biomedical Research and Innovation / RIKEN Center for Developmental Biology

2-2 Minatojima-Minamimachi, Chuo-ku, Kobe 650-0047

Phone: +81-78-304-5772 Fax: +81-78-304-5263

E-mail: Asa777@aol.com

Conflict of interest

All authors have no conflicts of interest.

Abstract

Failures in fracture healing are mainly caused by a lack of vascularization. Adult human circulating CD34+ cells, an endothelial/hematopoietic progenitor-enriched cell population, have been reported to differentiate into osteoblasts (OBs) in vitro, however the therapeutic potential of CD34+ cells for fracture healing is still unclear. Therefore, we performed a series of experiments to test our hypothesis that functional fracture healing is supported by vasculogenesis and osteogenesis via regenerative plasticity of CD34+ cells. Peripheral blood CD34+ cells, isolated from total mononuclear cells (MNCs) of adult human volunteers, showed gene expression of osteocalcin (OC) in 4 out of 20 freshly isolated cells by single cell RT-PCR analysis. Phosphate-buffered saline (PBS), MNCs or CD34+ cells were intravenously transplanted after creating non-healing femoral fractures in nude rats. RT-PCR and immunohistochemical staining at the peri-fracture site demonstrated molecular and histological expression of human-specific markers for endothelial cells and OBs at week 2. Functional bone healing assessed by biomechanical as well as radiological and histological examinations was significantly enhanced by CD34+ cell transplantation compared to the other groups. Our data suggest circulating human CD34+ cells have a therapeutic potential to prtomote an environment conducive to neovascularization and osteogenesis in damaged skeletal tissue, which will allow the complete healing of fractures.

Introduction

Whereas embryonic stem cells in the blastocyst stage have the ability to generate any differentiated cells in the body, most adult stem cells have limited potential for postnatal tissue/organ regeneration. Among phenotypically characterized adult stem/progenitor cells[1-3], the hematopoietic system has traditionally been considered as an organized, hierarchic system with multipotent, self-renewing stem cells at the top, lineage-committed progenitor cells in the middle, and lineage-restricted precursor cells, which give rise to terminally differentiated cells, at the bottom[4]. Recently, adult human peripheral blood CD34+ cells have been reported to contain intensive endothelial progenitor cells (EPCs) as well as hematopoietic stem cells (HSCs)[5] . Tissue ischemia and cytokine mobilize EPCs from bone marrow (BM) into peripheral blood, and mobilized EPCs specifically home to sites of nascent neovascularization and differentiate into mature endothelial cells (ECs) (vasculogenesis)[6,7]. In case of immunodificient rat model of acute myocardial infarction, transplanted human CD34+ cells or ex-vivo expanded EPCs incorporate into the site of the myocardial neovascularization, differentiate into mature ECs, augment capillary density, inhibit myocardial fibrosis and apoptosis, and preserve the left ventricular function[8-10]. In addition, intravenously transplanted CD34+ cells was efficiently incorporated into ischemic tissue[9,11].

In recent years, in an attempt to meet clinical demands, interest has turned to bone formation as an alternative category of regenerative medicine. It is anticipated that by optimizing the process of fracture repair, a biological approach results in the restoration of normal structure and function in the injured skeletal tissue. Although most fractures typically heal with callus formation which bridges the fracture gap, a significant proportion (5-10%) of fractures fail to heal and result in delayed union or persistent nonunion[12,13]. Inappropriate neoangiogenesis is considered to be a crucial factor in failed bone formation and remodeling[14,15]. Notably, appropriate vascularization is emerging as a prerequisite for bone

development and regeneration, and indeed there appears to be a developmental reciprocity between ECs and OBs[16]. Under such recognition, human CD34+ cells, which are capable of generating ECs in an appropriate environment[6,7], have also been reported to differentiate into OBs in vitro [17-19]. In addition, a recent report demonstrated that CD34+ osteoblastic cells line the cavities of the cartilage in the fracture site in a rabbit tibial osteotomy model[20]. These observations provoked the hypothesis that human peripheral blood CD34+ cells play a key role in fracture healing via vasuculogenesis and osteogenesis. Therefore, we first confirmed that mouse Sca1+Lineage marker- (Lin-) cells, quite similar to human CD34+ cells[7,21,22], were mobilized to peripheral blood in the natural course of the fracture healing process. Next, we investigated whether transplantation of circulating human CD34+ cells contributed to both vasculogenesis and osteogenesis for functional bone healing post-fracture in an immunodeficient rat model.

In the present series, we demonstrated that mouse Sca1+Lin- cells were mobilized into the peripheral blood in the natural course of fracture healing and that human peripheral blood CD34+ cells, containing osteo/endothelial progenitor cells already expressing OC, that were recruited to the fracture site following systemic delivery, developed a favorable environment for fracture healing by enhancing vasculogenesis and osteogenesis, and finally led to functional recovery from fracture. The present findings have important clinical implications for cell-based therapy that will enhance bone repair following fracture.

Materials and Methods

Isolation of mouse Lin- cells and assessment of Sca1+Lin- cells

To confirm the kinetics of Sca1+Lin- cells in the natural course of fracture healing, we detected Sca1+Lin- cells at pre-fracture and 1, 4, 7, 14 days post-fracture by fluorescence-activated cell sorting (FACS) analysis (n=3 in each).

Peripheral blood cells were aspirated from the hearts of 10-week-old fractured mice 1, 4, 7, 14 days post-fracture, and from those of unfractured mice with PBS containing 5% fetal calf serum (FCS) (n=3 in each). MNCs were obtained by a Histopaque-1083 (Sigma) density gradient centrifugation at 400g for 20 min. The light-density MNCs were collected, washed twice with Dulbecco's PBS supplemented with 2 mM EDTA and counted manually. Separation of Lin- cells was performed to deplete mature hematopoietic cells[7,21] such as T cells, B cells, NK cells, monocytes/macrophages, granulocytes and erythrocytes by labeling MNCs with lin- separation kit (BD Pharmingen), containing biotin-conjugated Mac1, B220, CD3e, Ter119, Ly6G, and CD45R antibodies followed by streptavidin-conjugated magnetic beads and BD IMagnet separation. Then, Lin-MNCs were counted and the number of Sca1+Lin- cells were calculated from the rate of Sca1+ cells in Lin- MNCs by FACS analysis and the number of Lin- MNCs.

Isolation of CD34+ cells from adult human volunteers

Human peripheral blood total MNCs were obtained from healthy male volunteers aged 31.7±1.2 years (n=3). CD34+ cells were isolated from the MNCs by the AutoMACS system (Miltenyi Biotec,. Auburn, CA) using anti-CD34 microbeads (Miltenyi Biotec). The CD34+ cell fraction had a purity of > 97%, as determined by FACS analysis using a CD34-specific monoclonal antibody (Becton Dickinson, San Jose, CA). IRB approval for the collection of peripheral blood MNCs from healthy human volunteers

and informed consent regarding the experimental use of the cells from the volunteers were obtained.

Flow cytometry studies and monoclonal antibodies

Regular flow cytometric profiles were analyzed with a FACS Calibur analyzer and CELLQuest software (Becton Dickinson Immunocytometry Systems, Mountain View, CA). The instrument was aligned and calibrated daily using a four color mixture of CaliBRITE beads (BD Biosciences) with FACSComp software (BD Bioscience). Dead cells were excluded from the plots beads on propidium iodide (PI) staining (Sigma Co., St. Louis, MO). Human CD34+ cells or mouse Lin- cells were washed twice with HBSS containing 3.0% FCS, incubated with 10 μl of FcR Blocking Reagent to increase the specificity of monoclonal antibodies (Miltenyi Biotic) for 20 min at 4°C, and incubated with the monoclonal antibodies for 30 min at 4°C. The stained cells were washed three times with PBS containing 3.0% FCS, and resuspended in 0.5 ml of HBSS/ 3%FCS/ PI, and analyzed by FACScan Caliber flow cytometer (Becton-Dickinson, Franklin Lakes, NJ). One hundred thousand cells were processed through the cytometer and 3 x 10^4 cells per sample were analyzed for human CD34+ cell or mouse Lin- cell fraction. The following monoclonal anti-human antibodies were used to characterize the CD34+ cell population: CD34-APC (BD Pharmingen), CD34-FITC (BD Pharmingen), CD45-FITC (BD Pharmingen), CD133-APC (BD Pharmingen), c-Kit-FITC (Nichirei), CD31-FITC (BD Pharmingen), CD105 (BD Pharmingen), VE cadherin (VE-cad)-FITC (BD Pharmingen), KDR-PE (BD Pharmingen), Tie2-PE (BD Pharmingen), IgG1-FITC isotype controls (BD Pharmingen), IgG1-APC isotype controls (BD Pharmingen), PI (Sigma Co., St. Louis, MO). The following monoclonal anti-mouse antibodies were used to characterize the Lin- MNCs: cKit-APC (BD Pharmingen), Sca1-FITC (BD Pharmingen), IgG2a-PE isotype controls (BD Pharmingen), IgG2a-FITC isotype controls (BD Pharmingen), PI (Sigma Co., St. Louis, MO).

Induction of femoral fracture with the periosteum cauterized and cell transplantation

Female athymic nude rats (F344/N Jcl rnu/rnu, CLEA Japan, Inc.) aged 8 to 12 weeks and weighing 150-170 g were used in this study. The rats were fed a standard maintenance diet and provided with water adlibitum. The institutional animal care and use committees of RIKEN Center for Developmental Biology approved all animal procedures including human cell transplantation.

All surgical procedures were performed under anesthesia and normal sterile conditions. Anesthesia was performed with ketamine hydrochloride (60 mg/kg) and xylazine hydrochloride (10 mg/kg) administered intraperitoneally. A lateral parapatellar knee incision on the right limb was made to expose the distal femoral condyle. An animal model of femoral fracture was applied using a modification of the method described by Bonnarens and Einhorn [23] . To avoid significant displacement of the fracture by obtaining the well aligned stability of the fracture site, a 1.2 mm diameter K-wire was inserted from the trochlear groove into the femoral canal in a retrograde fashion using a motor-driven drill. The wire was advanced until its proximal end was positioned stably in the greater trochanter and the distal end was cut close to the articular surface of the knee. A thin saw cut at depth of a 3 mm was applied mid-shaft following minimal lateral exposure to weaken the bone and to avoid complex fractures. A transverse femoral shaft fracture was then created in the right femur of each rat using a C-shaped instrument applying three-point bending. Following this procedure, each rat received additional surgery to create a nonunion in the fractured shaft according to the method of Kokubu, et al[24]. The periosteum was cauterized (OPTEMP™, Variable low temp cautery, Alcon Manufactureing, Ltd., U.S.) circumferentially at a distance of 2 mm on each side of the fracture. The wound was then irrigated with 10 cc of sterile saline and the muscle and skin were closed in layers with 5-0 nylone sutures. Post-operative pain was managed by administration of subcutaneous injection of buprenorphine hydrochloride after surgery. Unprotected weight bearing was allowed immediately post-operation. The left unfractured femur was served as a control.

Thirty minutes after the creation of the fracture model, rats received intravenous transplantation of 1x 10^5 CD34+ cells or 1x 10^5 total MNCs resuspended with 100 ul of PBS or the same volume of PBS without cells through their tail vein (n=15 in each group).

Three rats were randomly selected from each group and sacrificed for the histological study after radiological evaluation of fracture healing at each time point, at weeks 2, 4 and 8. The six remaining rats in each group were sacrificed at week 8 for biomechanical testing as described below. If the fracture was not a stable transverse fracture or if any evidence of deep infection was seen, the animals were excluded from the study and replaced with additional animals. Thus, eight rats with comminuted fractures and six rats with infection identified by radiographs were replaced during the experiment.

Targeting cell analysis with Qtracker cell labeling kit

To target human CD34+ cells or MNCs following intravenous infusion and confirm their recruitment into fracture site, Qtracker 655 cell labeling kit (Quantum Dot Corporation) was applied for the human cells prior to transplantation in three additional rats in each group according to the manufacturer's instructions. In brief, Qtracker cell labeling kits deliver fluorescent Quantum dot (qdot) nanocrystals into the cytoplasm of live cells using a custum targeting peptide and the long-term stability and brightness of qdots make them ideal candidates for live cell targeting and imaging [25,26]. The 1x10^5 CD34+ cells or MNCs were incubated for 60 minutes with the Qtracker labeling solution (1 μl Qtracker regent A and B) and 0.2 ml Dulbecco's modified Eagle's medium (DMEM) in 8-well Lasb-Teck chambered coverglass system. The cells were washed twice with DMEM and cell labeling was confirmed under fluorescence microscopy. The labeled cells were intravenously transplanted into each animal 30 minutes after fracture. All animals were sacrificed at day 7 for targeting cell analysis with Qtracker.

RT-PCR analysis of RNA isolated from CD34+ cells and peri-fracture site tissue

Total RNA was obtained from the human CD34+ cells immediately after isolation and from the rat tissues in peri-fracture site at day 14 using Tri-zol (Life Technologies) according to the manufacturer's instructions. The first-strand cDNA was synthesized using the RNA LA PCR Kit Ver 1.1 (Takara), amplified by Taq DNA polymerase (Advantage–GC cDNA PCR Kit, Clontech and AmpliTaq Gold DNA polymerase, Applied Biosystems). PCR was performed using a PCR thermalcycler (MJ research PTC-225). Human CD31 (hCD31), human VE-cadherin (hVE-cad), human Osteocalcin (hOC), human Collagen1A1 (hCol1A1), human vascular endothelial growth factor (hVEGF), human fibroblast growth factor 2 (hFGF2) and human hepatocyte growth factor (hHGF) were amplified by Taq DNA polymerase (Advantage–GC cDNA PCR Kit, Clontech) in the following conditions: 35 cycles of 30-second initial denaturation at 94°C, annealing at 56°C for 1 minute, and 30 seconds of extension at 72°C according to the manufacturer's instructions. Subsequently, PCR products were visualized in 1.5% ethidium bromide-stained agarose gels. Human umbilical vein endothelial cells (HUVECs) and hOBs (NHOst cells; Cambrex Bio Science, Walkersville Inc., Walkersville, MD) were used for the positive control for human-specific endothelial and bone-related genes.

Primers: To avoid interspecies cross-reactivity of the primer pairs between human and rat genes, we designed following human-specific primers using Oligo software (Takara). None of the primer pairs showed any cross-reactivity to rat genes (data not shown).

hCD31 primer sequence (363 bp): sense ATC GAT CAG TGG AAC TTT GCC TAT T; antisense GTG GCA TTT GAG ATT TGA TAG A

hVE-cad primer sequence (461 bp): sense ACG CCT CTG TCA TGT ACC AAA TCC T; antisense GGC CTC GAC GAT GAA GCT GTA TT

hOC primer sequence (417 bp): sense AAG CAA GTA GCG CCA ATC T; antisense GGA AGT AGG GTG CCA TAA CAC

hCol1A1 primer sequence (502 bp): sense CCT GGC CCC ATT GGT AAT GTT; antisense CCC

CCT CAC GTC CAG ATT CAC

h VEGF primer sequence (186 bp): sense CAA CAT CAC CAT GCA GAT TAT GC; antisense CCA CAG GGA CGG GAT TTC TTG

hFGF2 primer sequence (282 bp): sense AGC ACA GTA ACA CTA TCC TGC A; antisense AAA CGG AAA CGC TCA CCA TAA

hHGF primer sequence (282 bp): sense ACG AAC ACA GCT ATC GGG GTA; antisense CAT CAA AGC CCT TGT CGG GAT

hGAPDH primer sequence (596 bp): sense CTG ATG CCC CCA TGT TCG TC; antisense CAC CCT GTT GCT GTA GCC AAA TTC G

rGAPDH primer sequence (320 bp): sense GTG CCA GCC TCG TCT CAT AGA; antisense CGC CAG TAG ACT CCA CGA CAT

Single-cell PCR

Single-CD34+ cells derived from peripheral blood using MACS system were put individually into PCR tubes with 4.5 μl lysis buffer containing 50 mM Tris-HCl, 75 mM KCl, 5 units SuperRNaseIN (Ambion), 7.5 units PrimeRNase Inhibitor (Eppendorf), 0.5% NP40, 1 mM DTT, 50 μM dNTP, and 15 nM MO-dT30 primer (AAGCAGTGGTATCAACGCAGAGTGGCCATTACGGCCGTACTT-$(dT)_{30}$). Tubes were then incubated at 65°C for 2 minutes and cooled to 45°C for 2 minutes. Reverse transcription was then carried out by the addition of 100 units of SuperScriptIII (Invitrogen). After incubation at 45°C for 15 minutes, the reaction was terminated by heating at 65°C for 10 minutes. Next, 1.5 μl of RNA digestion mixture, 2 units RNaseH (Invitrogen) and 25mM $MgCl_2$, was added into each tube and RNA digestion was performed by incubating at 37°C for 15 minutes, and then inactivating at 65°C for 10 minutes. Following RNA digestion, 6.5 μl of reaction mixture [5 X Terminal transferase buffer (Roche), 3mM $CoCl_2$, 1.5mM dATP, and 15 units TdT (Promega)] was added and poly (A) tailing performed by

incubating at 37°C for 15 minutes, and inactivation was carried out at 65°C for 10 minutes. cDNA amplification was carried out using ExTaq polymerase (Takara Biochemicals, Japan). Briefly, polyA-tailed cDNA (13μl) was split 4 μl each into two tubes containing 16 μl of primary PCR reaction solution containing ExTaq PCR buffer (Takara Biochemicals), 2 mM dNTP, 10 μM MO-dT30 primer and 1 units of ExTaq polymerase (Takara Biochemicals). PCR was performed with one cycle of 1 minute at 94°C, 2 minutes at 50°C and 2 minutes at 72°C, followed by 35 cycles of 30 seconds at 94°C, 30 seconds at 60°C, and 2 minutes at 72°C. After combining split tubes into one tube, 2 μl of 1st amplified cDNA was added to 18 μl of 2nd PCR mixture, ExTaq PCR buffer (Takara Biochemicals), 2 mM dNTP, 2 μM MO-dT30 primer and 1 units of ExTaq polymerase (Takara Biochemicals), and 2nd PCR was performed 35 cycles of 30 seconds at 94°C, 30 seconds at 60°C, and 2 minutes at 72°C. Finally, amplified cDNA purified with Qiagen PCR purification kit according to manufacturer's procedure and then PCR analysis for specific gene expression was carried out using each purified cDNA.

Primers: hCD34 primer sequence (91 bp): sense TGC CTC TTC TGT GGG TGA CC; antisense TCC AAC CGT CAT TGA AAC CAG

hOC primer sequence (96 bp): sense GCT CAA TCC GGA CTG TGA CG; antisense CAG AGC GAC ACC CTA GAC CG

hGAPDH primer sequence (95 bp): sense GCA TTG CCC TCA ACG ACC; antisense CAT GTG GGC CAT GAG GTC C

Tissue harvesting

Rats were euthanized with an overdose of ketamine and xylazine. Bilateral femurs were harvested and quickly embedded in OCT compound (Miles Scientific, Elkhardt, IN), snap frozen in liquid nitrogen, and stored at -80°C for histochemical and immunohistochemical staining as described below. Rat femurs in OCT blocks were sectioned, and 6 μm serial sections were mounted on silane-coated glass slides and

air dried for 1 hour before being fixed with 4.0 % paraformaldehyde at 4°C for 5 minutes and stained immediately.

Morphometric evaluation of capillary density and osteoblast density

Histochemical staining (n=3 in each group) for isolectin B4 (Vector Laboratories) as a rat EC marker or OC (Santa Cruz Biotechnology) as a rat OB marker was visualized with DAB (Vector Laboratories), and capillary or osteoblast density was morphometrically evaluated as the average value in 5 randomly selected fields of soft tissue in the peri-fracture site (Figure 3M, *a* and *b*). To address the location of chondrocytes in the fractured sections, toluisine blue was used for counter staining. Capillaries were recognized as tubular structures positive for isolectin B4. OBs were recognized as lining or floating cells positive for OC on new bone surface. All morphometric studies were performed by two examiners blind to treatment.

Physiological assessment of tissue perfusion by Laser Doppler Perfusion Imaging

Laser Doppler Perfusion Imaging (n=3 in each group) (LDPI, Moor Instrument, Wilmington, DE) [27,28] was used to measure serial blood flow in both legs over the course of 2 weeks post-fracture. The ratio of fractured / intact (contralateral) blood flow was calculated to evaluate the serial blood flow recovery after fracture. The measurement was done under anesthesia with the animals supine and both limbs fully extended.

Immunofluorescent staining

To detect transplanted human cells in the rat fracture site, immunohistochemistry (n=3) was performed with following human-specific antibodies; human leukocyte antigen (HLA)-ABC (BD Pharmingen) to detect various kind of human cells, hCD31 (DAKO) for human ECs and hOC

(Biogenesis) for human OBs. Staining specificity for human cells without cross reaction to rat cells was confirmed by histochemical staining for HLA-ABC, hCD31 and hOC using human and rat heart or bone samples (data not shown). Double immunohistochemistry with HLA-ABC or hCD31 and smooth muscle actin (SMA) was performed to detect various human cells or human ECs in the arterioles. To estimate how many intravenously injected cells had recruited to the fracture site, the number of HLA-ABC-positive cells was morphometrically counted as the average value in five randomly selected soft tissue fields in the peri-fracture site. The secondary antibodies for each immunostaining were as follows; Alexa Flour 594-conjugated goat anti-mouse IgG_1 (Molecular Probes) for HLA-ABC and hCD31 staining and Alexa Flour 488-conjugated goat anti-mouse IgG_{2a} (Molecular Probes) for SMA. Immunohistochemistry with hOC was performed to detect human OBs along the newly formed bone surface. The secondary antibodies for hOC is Cy3-conjugated affinipure goart anti-rabbit IgG (H+L) (Jackson ImmunoResearch). DAPI solution was applied for 5 minutes for nuclear staining.

Inhibition of neovascularization

To investigate the hypothesis that neovascularization is essential for supporting endogenous bone regeneration, we used an antiangiogenic agent, soluble (s) Flt1 (VEGF receptor 1), known to inhibit proliferation of endothelial cells[29]. First, we investigated whether transplanted human CD34+ cells released angiogenic factors (hVEGF, hFGF2, hHGF) at the fracture site compared to the MNCs. Next, rats subjected to fracture and CD34+ cell transplantation were divided into two groups; one group receiving sFlt1 (20 ug/kg; subcutaneous; R&D systems) once daily for 14 days and the other receiving PBS only (n=3 in each group). On day 14 after the cell transplantation, capillary and OB density, blood flow and callus formation were assessed in each group.

Radiographic assessment of the fracture healing

Radiographs of the fractured legs were serially taken at weeks 0, 2, 4 and 8, under anesthesia with the animal supine and both limbs fully extended. Fracture union was identified by the presence of bridging callus on two cortices. Radiographs of each animal were examined by three observers blind to treatment.

To evaluate the fracture healing process, callus formation was monitored radiographically and relative callus areas detected by radiography were quantified with NIH image at week 2 in all groups.

Histological assessment of the fracture healing

Histological evaluation (n=3 in each group) was performed with toluidine blue staining to address the process of endochondral ossification at weeks 2, 4 and 8.

The degree of fracture healing was evaluated at week 2, 4, and 8 in each group using a five point scale proposed by Allen et al[30] as following: Grade 4, complete bony union; Grade 3, an incomplete bony union (presence of a small amount of cartilage in the callus), Grade 2, a complete cartilaginous union (well-formed plate of hyaline cartilage uniting the fragments) , Grade 1, an incomplete cartilaginous union (retention of fibrous elements in the cartilaginous plate), and Grade 0, the formation of a pseudoarthrosis (most severe form of arrest in fracture repair). All morphometric studies were performed by 2 orthopedic surgeons blind to treatment.

Biomechanical assessment of the fracture union

At week 8, six rats in each treatment group were used for biomechanical evaluation [31-34]. Following euthanization, the fractured femurs and the contralateral nonfractured intact femurs were dissected free from the surrounding muscle. After the intramedullary K-wires were removed, a standardized three-point bending test was performed on the fractured site and the same portion of the intact contralateral femur using a load torsion and bending tester (Computer Control System Shimazu

Autograft, Simazu Co., Kyoto, Japan). The bending force was applied with cross-head at a speed of 2 mm/min until fracture occurred. The ultimate stress (N/mm^2), the extrinsic stiffness (N/mm) and the failure energy (Nmm) were interpreted and calculated from the load deflection curve, which was recorded continuously in the computerized monitor linked to the tester. The percentage ratio of each parameter in the fractured (right) femur versus un-fractured (left) femur was calculated in each animal.

Statistical Analysis

All values were expressed as mean ± SE. Paired t tests were performed for comparison of data before and after treatment. The comparisons among three groups were made using the one-way analysis of variance (ANOVA). Post hoc analysis was performed by Fisher's PLSD test. A probability value <0.05 was considered to denote statistical significance.

Results

Augmented mobilization of mouse Sca1+Lin- cells by fracture stress

To confirm the kinetics of peripheral blood mouse Sca1+Lin- cells in the natural course of fracture healing, we serially performed FACS analysis to assess number of Sca1+Lin- cells in the peripheral blood post-fracture. The MNCs obtained from the mice were $38.9\pm4.8\times10^4$ cells and the number of Lin-MNCs after Lineage maker depletion by MACS system was $26.5\pm3.0\times10^4$ cells. The percentage of peripheral blood Sca1+ Lin- cells in relation to Lin- MNCs by FACS analysis had a tendency to peak at day 1 post-fracture and gradually decrease thereafter, however these changes were not statistically significant (pre-fracture, 45.4±0.6; 1 day post-fracture, 59.3±3.1; 4 days post-fracture, 57.7±1.1; 7 days post-fracture, 54.3±1.0; 14 days post-fracture, 52.6±2.4%) (Fig.1A). The number of Sca1+Lin- cells, calculated from the number of Lin- MNCs and the percentage of Sca1+ cells in the

number of Lin- MNCs, significantly increased at day 1 post-fracture and then gradually decreased (pre-fracture, 8.3±1.4; 1 day post-fracture, 22.1±6.1; 4 days post-fracture, 15.6±9.7; 7 days post-fracture, 12.9±5.7; 14 days post-fracture, 8.4±1.9 $x10^4$ cells/ml. $P<0.05$ for pre-fracture vs 1 day post-fracture) (Fig. 1B).

These results indicate that mouse Sca1+Lin- cells, quite similar to human CD34+ cells, were mobilized into the peripheral blood at an early phase of the fracture healing process.

Phenotypic characterization of CD34+ cells obtained from adult human volunteers

Peripheral blood total mononuclear cells (MNCs) were obtained from healthy male volunteers aged 31.7±1.2 years (n=3) and CD34+ cells were isolated from the MNCs by AutoMACS. The MNCs contained a CD34+ cell fraction at the rate of < 0.5% and the CD34+ cell fraction had a purity of > 97% as determined by FACS analysis (Fig. 2A). The freshly isolated CD34+ cells were also characterized as positive for cell surface markers of CD45, CD133, c-Kit, CD31 and CD105 (Fig. 2B). RT-PCR analysis of the CD34+ cells revealed weak expression of the human-specific genes, hCD31 and hOC, but not of another EC marker, hVE-cad, and another bone-related marker, hCol1A1 (Fig. 2C, D). RT-PCR analysis at the single cell level of the CD34+ cells revealed that 4 out of 20 CD34+cells expressed hOC (Fig.2E).

These results indicate that human peripheral blood CD34+ cells contain not only endothelial progenitor but also osteo-progenitor cells [19, 35].

Massive recruitment of CD34+ cells into the fracture site

To simulate the clinical situation of the non-healed fracture, a reproducible model of femoral fracture [23] with cauterized periosteum, which led to nonunion 8 weeks post-fracture[12,24], was applied in nude rats. Human CD34+ cells isolated from peripheral blood were labeled with the Qtracker cell labeling kit (Qtracker, Quantum Dot Corporation) and intravenously administered via the tail vein 30

minutes after fracture creation. MNCs labeled with Qtracker or PBS alone was similarly infused into control animals. Rats were sacrificed 1 week after the cell infusion and then histochemical staining for isolectin B4, a rat-specific EC marker, was performed. Fluorescent microscopy demonstrated a massive recruitment of human cells with tubular structure, which were morphologically compatible with vascular cells, and the enhancement of neovascularization by rat ECs around the granulation area (*zone a* in Fig. 3M) in animals treated with CD34+ cells (CD34+ group) (Fig. 3A). In contrast, recruitment of human cells into this area was rarely observed in rats receiving MNCs, and augmentation of recipient vascularity was not obvious in animals receiving MNCs or PBS (Fig. 3B, C). To further confirm the human cell incorporation into the fracture site, especially into the arterioles, tissue samples were stained with HLA-ABC and SMA. The double immunostaining demonstrated the massive recruitment of the human cells in the granulation area with relatively rare incorporation along the inner layer of SMA–positive smooth muscle cells in CD34+ group. The human cells lining along the inner layer were morphologically compatible with endothelial cells (Fig. 3D). In contrast, less recruitment of human cells in the granulation area and no human cells along the inner layer of arterioles were observed in animals receiving MNCs (Fig. 3E). No human cells were found in the area of PBS group (Fig. 3F). The number of human cells in the granulation area was significantly higher in the CD34+ group compared with the other groups (CD34+, 93.1±11.3; MNC, 43.1±10.4; PBS, 0.0±0.0 /mm^2, respectively. $P<0.01$ for CD34+ vs MNC or PBS group) (Fig. 3O).

Fluorescent microscopy 1 week after the cell infusion also demonstrated abundant recruitment and distribution of human cells in the newly bone formed area (*zone b* in Fig. 3M) as well as the granulation area in CD34+ group (Fig. 3G). In contrast, recruitment of human cells into *zone b* was rarely observed in other groups (Fig. 3H, I). To quantitatively assess the number of recruited cells, tissue samples were stained with HLA-ABC and the number of HLA-ABC-positive cells was morphometrically counted in the newly bone formed area. Fluorescent microscopy demonstrated a massive recruitment of

human cells in CD34+ group (Fig. 3J). In contrast, there was less recruitment of HLA-positive cells in animals receiving MNCs (Fig. 3K) and no human cells were seen in the PBS group (Fig. 3L). The number of HLA-ABC-positive cells in the newly bone formed area was significantly greater in the CD34+ group compared with the other groups (CD34+, 84.7±13.5; MNC, 47.2±9.0; PBS, 0.0±0.0 /mm^2 respectively. $P<0.05$ for CD34+ vs MNC, $P<0.01$ for CD34+ vs PBS group) (Fig. 3P).

These morphological findings indicate that human peripheral blood CD34+ cells infused intravenously are recruited into not only the granulation zone but also the newly bone formed zone in the fracture healing process.

Human CD34+ cell-derived vasculogenesis and osteogenesis

Next, we performed experiments to characterize the human cells recruited into the fracture sites. To histologically prove the phenomenon of human cell-derived vasculogenesis, immunohistochemical staining for hCD31, a human-specific EC marker, was performed using tissue samples obtained 2 weeks after cell infusion. Differentiated human ECs derived from the transplanted CD34+ cells were detected as hCD31+ cells in the vasculature in the peri-fracture area (Fig. 4A, D), while hCD31+ cells were not identified in the MNC (Fig. 4B) or PBS group (Fig. 4C). To further confirm this phenomenon in terms of transcription, RT-PCR analysis of tissue RNA isolated from the peri-fracture site was performed. The molecular approach revealed the gene expression of human-specific EC markers (hCD31 and hVE-cad) in the CD34+ group, but not in the other groups (Fig. 4E).

To identify human cell-derived osteogenesis, immunohistochemical staining for hOC, a human-specific OB marker was performed using tissue samples obtained 2 weeks after cell infusion. Human OBs derived from the transplanted CD34+ cells were observed as lining cells along the newly formed bone surface (Fig. 4F, I), while only a few human OBs were identified in the MNC group (Fig. 4G) and no human OBs were identified in the PBS group (Fig. 4H). RT-PCR analysis of tissue RNA

isolated from the peri-fracture site demonstrated the expression of human-specific bone-related markers (hOC and hCol1A1) in the CD34+ group, but not in other groups (Fig. 4J).

These results indicate that human peripheral blood CD34+ cells differentiate into both ECs and OBs in a fracture-induced environment.

Enhancement of intrinsic angiogenesis and osteogenesis in animals receiving CD34+ cells

Enhanced angiogenesis and osteogenesis by recipient's cells following cell transplantation were further confirmed by immunostaining for rat-specific markers. Vascular staining with isolectin B4 (marker for rat EC, but not human) using tissue samples at week 2 post-fracture demonstrated enhanced neovascularization around the granulation area (*zone a* in Fig. 3M) in CD34+ group compared with MNC or PBS group (Fig. 5A). Neovascularization assessed by capillary density was significantly enhanced in CD34+ group compared with the other groups (CD34+, 1187.5±79.3; MNC, 562.5±36.6; PBS, 532.5±49.3 /mm^2, respectively. $P<0.01$ for CD34+ vs MNC or PBS group) (Fig. 5A).

OB staining for rat-specific OC (marker for rat OB but not human) using tissue samples at week 2 post-fracture revealed augmentation of osteogenesis in the area of new bone formation (*zone b* in Fig. 3M) in animals treated with CD34+ cells compared with those receiving MNCs or PBS alone (Fig. 5C). Osteogenesis assessed by the OB density was significantly enhanced in CD34+ group compared with other groups (CD34+, 468.0±25.3; MNC, 321.6±28.8; PBS, 141.6±14.0 /mm^2, respectively. $P<0.01$ for CD34+ vs MNC or PBS group) (Fig. 5C).

These results indicate that administration of human CD34+ cells enhances both intrinsic angiogenesis and osteogenesis by recipient cells.

Improvement of blood flow and enhancement of callus formation in animals receiving CD34+ cells after fracture

To evaluate blood flow recovery at the fracture site by physiological approach, LDPI was serially performed after fracture. LDPI analysis demonstrated severely low blood flow at the fracture sites 1 hour after fracture creation and its recovery at week 2 in all groups (Fig. 5B). The ratio of fractured / intact (contralateral) blood flow was significantly increased by week 2 in all groups (Fig. 5B). There was no significant difference in the blood flow ratio 1 hour after fracture creation among the groups, while the ratio at day 14 was significantly higher in CD34+ group compared with the other groups (CD34+, 1.344±0.079; MNC, 1.096±0.037; PBS, 1.085±0.024, respectively. $P<0.05$ for CD34+ vs MNC or PBS group) (Fig.5B).

To evaluate the fracture healing process, callus formation was monitored radiographically and the relative callus area detected by radiography was quantified with NIH image at week 2 in all groups (Fig. 5D). The relative callus area was significant larger in CD34+ group compared with the other groups (CD34+, 13.67±1.76; MNC, 7.00±0.57; PBS, 5.00±1.15, respectively. $P<0.05$ for CD34+ vs MNC or PBS group) (Fig. 5D).

These results indicate that administration of human peripheral blood CD34+ cells contribute to improvement of tissue perfusion and enhancement of bone formation following fracture.

Inhibitionn of intrinsic angiogenesis and osteogenesis by antiangiogenic agent in animals receiving CD34+ cell transplantation

At first, we confirmed that transplanted human CD34+ cells released a greater amount of angiogenic factors (hVEGF, hFGF2, hHGF) than the MNCs at the fracture site (Fig. 6A), Next, to investigate the hypothesis that neovascularization is essential to support endogenous bone regeneration after CD34+ cell infusion, we used an antiangiogenic agent, sFlt1. Rat-specific vascular staining with isolectin B4 at week 2 demonstrated reduced capillary density in *zone a* in animals treated with CD34+ cells and sFlt1 compared with those receiving CD34+ cells and PBS (sFlt1, 908.3±90.6; PBS,

1258.3±69.1/mm^2, respectively. P<0.05 for sFlt1 vs PBS group) (Fig. 6B). The skin blood flow within the fractured site and the intact contralateral site were calculated by LDPI. By week 2, the ratio of fractured / intact contralateral blood flow was significantly reduced in the sFlt1 treated group compared to the PBS group (sFlt1, 1.180±0.096; PBS, 1.428±0.159, respectively. P<0.05 for sFlt1 vs PBS group) (Fig. 6C).

Rat-specific OC staining at week 2 revealed a reduction of OB density, a parameter of intrinsic osteogenesis, in *zone b* in animals treated with CD34+ cells and sFlt1 compared to those receiving CD34+ cells and PBS (sFlt1, 352.0±17.3; PBS, 440.7±30.0/mm^2, respectively. P<0.05 for sFlt1 vs PBS group) (Fig. 6D). The relative callus area assessed by radiograph at week 2 was significant smaller in sFlt1 treated group compared to PBS group (sFlt1, 7.33±0.67; PBS, 12.33±1.53, respectively. P<0.05 for sFlt1 vs PBS group) (Fig. 6E).

These findings indicate that the administration of human CD34+ cells contributed in an autocrine/paracrine manner to fracture healing by releasing angiogenic factors.

Morphological and functional recovery of fractured bone in animals receiving CD34+ cell transplantation

Morphological recovery of fractured bone in each group was evaluated by radiographic and histological examinations. In 66 percent of rats (9 of 12) at week 4 and all rats at week 8 (9 of 9) in the CD34+ group, the fracture radiographically healed with bridging callus formation, while the fracture site in the other groups showed no bridging callus formation and resulted in nonunions, consistent with a previous report showing the natural course of this animal model[20] (Fig. 7A). Histological evaluation with toluidine blue staining demonstrated enhanced endochondral ossification consisting of numerous numbers of chondrocytes and newly formed trabecular bone at week 2, bridging callus formation at week 4, and complete union at week 8 in CD34+ group (Figure 7B). In contrast, although a thick callus

formation was observed at week 2, the healing process had stopped by week 4 and finally the callus was absorbed at week 8 in the other groups (Fig. 6B). The degree of fracture healing assessed by Allen's classification[25] was significantly higher value in CD34+ group compared with other groups at week 4 and 8 (2W: CD34+, 1.3±0.3; MNC, 0.7±0.3; PBS, 0.3±0.3, not significant for CD34+ vs other groups, 4W: CD34+, 2.3±0.3; MNC, 0.3±0.3; PBS, 0.3±0.3, $P<0.05$ for CD34+ vs other groups, 8W: CD34+, 3.7±0.3; MNC, 0.0±0.0; PBS, 0.0±0.0, $P<0.01$ for CD34+ vs other groups, respectively.) (Fig. 7C).

Furthermore, to confirm the functional recovery of the fractured bone, biomechanical evaluation by a three-point bending test was performed at week 8 in all groups. Specimen length was similar in CD34+ cell group (15.2±1.9 mm), MNC group (15.5±2.1mm) and PBS group (14.8±1.3 mm). The percent ratios of all parameters in the fractured femur versus contralateral intact femur in CD34+ group were significantly superior to those in the other groups (%ultimate stress: CD34+, 112.3±5.3; MNC, 25.5±8.3; PBS, 13.1±4.3%, $P<0.01$ for CD34+ vs other groups, %extrinsic stiffness: CD34+, 121.1±8.1; MNC, 12.1±3.8; PBS, 6.8±2.6%, $P<0.01$ for CD34+ vs other groups; %failure energy: CD34+, 127.3± 12.1; MNC, 57.3± 10.7; PBS, 40.3± 8.2%, $P<0.05$ for CD34+ vs other groups) (Fig. 7D).

These results indicate that the femoral fractures with cauterized periosteum in the immunodeficient rats were morphologically and functionally healed by the administration of human peripheral blood CD34+ cells.

Discussion

Severe skeletal injury accompanied by fracture and loss of blood supply results in delayed union or established nonunion. Recovery of blood flow at the injury site is considered to be essential for adequate fracture healing[15,16]. Therefore, appropriate neovascularization is emerging as a prerequisite for bone development and regeneration through developmental reciprocity between ECs and OBs[16]. One of

the most promising approaches for overcoming this clinical issue is by grafting the vascularized bone, however, this process requires painstaking microvascular surgical skill[12]. Thus, the development of a more practical strategy for fracture healing is required and many surgeons have begun looking at therapeutic neovascularization to answer this need. Recent advances in stem cell biology have suggested the feasibility and effectiveness of cell-based therapy. Human circulating CD34+ cells, EPC- and HSC-enriched fraction, have been shown to have therapeutic potential for ischemic diseases through vasculogenesis mechanism in our previous studies[5-7]. As we anticipated, mouse Sca1+Lin- cells, quite similar to human CD34+ cells, were mobilized into peripheral blood in the natural course of fracture healing and human CD34+ transplantation induced significant vasculogenesis in regenerating tissues and enhanced functional recovery from non-healing fracture in small animal models.

However, human CD34+ cells are reported to be not only hematopoietic and vasculogenic but also capable of differentiating into OBs in vitro[17-19]. Quite recent reports demonstrated that the murine BM side population (SP) cells, which contain hematopoietic repopulating cells[38], can engraft in bone after intravenous transplantation[39] and that a nonadhesive population of cultured BM cells contains primitive cells capable of generating into both hematopoietic and osteogenic lineages in vivo[40]. In addition, Ford et al recently reported that CD34+ osteoblastic cells line the cavities of the cartilage in the fracture site of rabbit tibial osteotomy model[20]. Although several reports suggest the commitment of HSC- or EPC-rich cell population into osteogenic lineage cells, the morphological and physiological incorporation of these cells for medical application has never been proved.

In the present study, we utilized a reproducible animal model of non-healing femur fracture with severe decrease in local blood flow, physiologically proven by LDPI examination. The natural history of this model is clearly relevant to the clinical situation of delayed union or nonunion. We identified in vivo multi-lineage plasticity of human peripheral blood CD34+ cells into OBs as well as ECs by not only immunohistochemistry but RT-PCR for human-specific cell markers. Recent reports demonstrated in vitro

or in vivo trans-lineage differentiation of CD34+ cells into cardiomyocytes[41-44], and peripheral blood CD34+ cells were also shown to contain a cell fraction expressing not only hematopoietic and endothelial, but also cardiac, skeletal, hepatic and neural lineage markers after G-CSF administration or myocardial ischemia[45,46]. However, the exact mechanism of the phenomena is not yet fully understood. Considering that CD34+ cells are EPC and HSC-enriched but still a heterogeneous cell population, there may be several possible mechanisms underlying the multi-lineage differentiation: 1) differentiation of original multipotent stem cells into multiple lineages; 2) differentiation of multiple kind of lineage-committed progenitor cells into each lineage; 3) transdifferentiation of hematopoietic/ endothelial lineage cells into mesenchymal lineage; 4) cell fusion between transplanted cells and recipient cells. The present RT-PCR results revealed a weak gene expression of human-specific OC in freshly-isolated human CD34+ cells, strongly supported by single-cell PCR analysis (before transplantation), and enhancement of the gene expression 14 days after transplantation. These findings indicate that CD34+ cell fraction contains a few multipotent stem and/or committing osteogenic progenitor cells, subsequently representing the osteogenic activity under the microenvironment of fracture. Enhbali-Fatourechi et al. quite recently demonstrated that sorted OC-positive cells in human peripheral blood formed mineralized nodules in vitro and bone in an in vivo transplantation assay[47]. Their novel report may support the hypothesis that CD34+ cell fraction contains a few osteo/endothelial progenitor cells, contributing to an enhanced functional recovery of the fracture.

In addition to these sensitive assessments of donor cell differentiation at the incorporated site, quantitative histochemical analysis for rat ECs and OBs revealed the enhancement of intrinsic angiogenesis and osteogenesis by recipient cells following the administration of human CD34+ cells. Human CD34+ cells were reported to secrete numerous angiogenic factors, including VEGF, HGF, FGF2 and IGF1 in vitro[36,37]. Our in vivo data also demonstrated that gene expression levels of human angiogenic factors including VEGF, FGF2 and HGF at the fracture site were greater in CD34+ cell group

compared with the MNC group. Moreover, we proved that the inhibition of angiogenesis by sFlt1 suppressed not only angiogenesis/vasculogenesis but also intrinsic osteogenesis, indicating that angiogenic factors released by the transplanted CD34+ cells, at least in part, contribute to fracture healing in paracrine manner. Although the detailed mechanism of the paracrine effect of human CD34+ cells is still unclear, a co-operative signal between HSCs/ EPCs and OBs may need to be further considered as a mechanism of multi-lineage regeneration by CD34+ cell transplantation. The niche regulating birth and differentiation of HSCs is known to consist of OBs, which line the inner surface of BM[48,49]. Zhang et al[50] reported that depleting the receptor of bone morphogenic protein (BMP) in OBs caused a doubling in both OB and HSC populations, offering same insight into the native of HSCs. Calvi et al[51] found the parallel expansion of HSCs when the number of OBs increased by parathyroid hormone infusion. In addition, Ponomaryov et al reported that immature OBs and ECs control homing, retention, and repopulation of SRC (severe combined immunodeficiency repopulating cells) by secreting SDF-1 as a host defence in response to DNA damage[52]. These findings indicate that osteogenesis and hematopoiesis/ vasculogenesis closely regulate each other in terms of microenvironmental interaction for regenerative activity in BM. Microenviromental interaction between osteogenic and vasculogenic lineage cells may involve not only paracrine regulatory factors, but also direct cellular communications in developing CD34+ cells. Enhanced angiogenesis/vasculogenesis signal could exert a cellular commitment and the development of CD34+ cells into the osteogenic lineage in response to a rigorous demand for skeletal tissue repair as a co-operative organogenesis mechanism.

The present results, showing the potential of CD34+ cells for multi-lineage plasticity, suggest that CD34+ cell transplantation contributes to forming an ideal local environment for fracture healing by supplying adequate blood flow and stimulating osteogenesis. The environmental contribution of CD34+ cells resulted in morphological and physiological healing of the fracture. Radiographic examination and histological toluidine blue staining demonstrated enhancement of endochondral ossification leading to

bridging callus formation only after CD34+ cell transplantation but not in the MNC and PBS groups. Finally, the biomechanical three-point bending test confirmed significant functional recovery from fracture following administration of CD34+ cells. These findings strongly suggest that peripheral blood CD34+ cells have significant potential for therapeutic application to the damaged skeletal tissue.

On the basis of preclinical achievements of cell-based therapy for injured bone[53] or osteogenesis imperfecta[54], transplantation of whole BM cells or BM mesenchymal stem cells has been clinically applied for bone/ cartilage regeneration[55,56]. It remains to be clarified whether circulating CD34+ cell transplantation is superior to the BM cell therapy in terms of efficacy and safety for fracture healing; however, cell harvest from peripheral blood dose provide positives in that (1) it is less invasive and safer than BM aspiration under general anesthesia, and (2) magnetic sorting of CD34+ cells has been clinically applied in the hematology field for many years[57,58]. The technical feasibility in a clinical situation and the present preclinical findings demonstrating morphological and functional fracture healing through concurrent vasculogenesis and osteogenesis strongly suggest promising results for the future clinical application of circulating CD34+ cells for non-healing fracture.

In conclusion, human circulating CD34+ cells have potent vasculogenic and osteogenic plasticity in the fracture-induced environment, enabling them to make a remarkable contribution to morphological and functional bone healing.

Acknowledgement

We thank Drs M. Osawa and S. Nishikawa (RIKEN CDB, Japan) for technical support with single-cell PCR. We thank Y. Masukawa and T. Itoh for secretarial assistance. We would like to thank Ms. Janina Tubby for her editing assistance in preparing for this manuscript.

References

1. Slack JM: Stem cells in epithelial tissues. Science 2000, 287:1431-1433
2. Blau HM, Brazelton TR, Weimann JM: The evolving concept of a stem cell: entity or function? Cell 2001, 105:829-841
3. Korbling M, Estrov Z: Adult stem cells for tissue repair - a new therapeutic concept? New Engl J Med 2003, 349:570-582
4. Weissman IL: Stem cells: units of development, units of regeneration, and units in evolution. Cell 2000, 100:157-168
5. Asahara T, Murohara T, Sullivan A, Silver M, van der Zee R, Li T, Witzenbichler B, Schatteman G, Isner JM: Isolation of putative progenitor endothelial cells for angiogenesis. Science 1997, 275:964-967
6. Asahara T, Masuda H, Takahashi T, Kalka C, Pastore C, Silver M, Kearne M, Magner M, Isner JM: Bone marrow origin of endothelial progenitor cells responsible for postnatal vasculogenesis in physiological and pathological neovascularization. Circ Res 1999, 85:221-228
7. Takahashi T, Kalka C, Masuda H, Chen D, Silver M, Kearney M, Magner M, Isner JM, Asahara T: Ischemia- and cytokine-induced mobilization of bone marrow-derived endothelial progenitor cells for neovascularization. Nat Med 1999, 5:434-438
8. Kawamoto A, Tkebuchava T, Yamaguchi J, Nishimura H, Yoon YS, Milliken C, Uchida S, Masuo O, Iwaguro H, Ma H, Hanley A, Silver M, Kearney M, Losordo DW, Isner JM, Asahara T: Intramyocardial transplantation of autologous endothelial progenitor cells for therapeutic neovascularization of myocardial ischemia. Circulation 2003, 107:461-468
9. Kocher AA, Schuster MD, Szabolcs MJ, Takuma S, Burkhoff D, Wang J, Homma S, Edwards NM, Itescu S: Neovascularization of ischemic myocardium by human bone-marrow-derived angioblasts prevents cardiomyocyte apoptosis, reduces remodeling and improves cardiac function.[see comment]. Nat Med 2001, 7:430-436
10. Kawamoto A, Gwon HC, Iwaguro H, Yamaguchi JI, Uchida S, Masuda H, Silver M, Ma H, Kearney M, Isner JM, Asahara T: Therapeutic potential of ex vivo expanded endothelial progenitor cells for myocardial ischemia. Circulation 2001, 103:634-637
11. Taguchi A, Soma T, Tanaka H, Kanda T, Nishimura H, Yoshikawa H, Tsukamoto Y, Iso H, Fujimori Y, Stern DM, Naritomi H, Matsuyama T: Administration of CD34+ cells after stroke enhances neurogenesis via angiogenesis in a mouse model. J Clin Invest 2004, 114:330-338

12. Rodriguez-Merchan EC, Forriol F: Nonunion: general principles and experimental data. Clin Orthop Relat Res 2004:4-12
13. Marsh D: Concepts of fracture union, delayed union, and nonunion. Clin Orthop Relat Res 1998:S22-30
14. Colnot CI, Helms JA: A molecular analysis of matrix remodeling and angiogenesis during long bone development. Mech Develop 2001, 100:245-250
15. Gerstenfeld LC, Cullinane DM, Barnes GL, Graves DT, Einhorn TA: Fracture healing as a post-natal developmental process: molecular, spatial, and temporal aspects of its regulation. J Cell Biochem 2003, 88:873-884
16. Karsenty G, Wagner EF: Reaching a genetic and molecular understanding of skeletal development. Dev Cell 2002, 2:389-406
17. Long MW, Williams JL, Mann KG: Expression of human bone-related proteins in the hematopoietic microenvironment. J Clin Invest 1990, 86:1387-1395
18. Chen JL, Hunt P, McElvain M, Black T, Kaufman S, Choi ES: Osteoblast precursor cells are found in CD34+ cells from human bone marrow. Stem Cells 1997, 15:368-377
19. Tondreau T, Meuleman N, Delforge A, Dejeneffe M, Leroy R, Massy M, Mortier C, Bron D, Lagneaux L: Mesenchymal stem cells derive from CD133 positive cells in mobilized peripheral blood and cord blood: proliferation, Oct-4 expression and plasticity. Stem Cells 2005
20. Ford JL, Robinson DE, Scammell BE: Endochondral ossification in fracture callus during long bone repair: the localisation of 'cavity-lining cells' within the cartilage. J Orthop Res 2004, 22:368-375
21. Otani A, Kinder K, Ewalt K, Otero FJ, Schimmel P, Friedlander M: Bone marrow-derived stem cells target retinal astrocytes and can promote or inhibit retinal angiogenesis. Nat Med 2002, 8:1004-1010
22. Rafii S, Lyden D: Therapeutic stem and progenitor cell transplantation for organ vascularization and regeneration. Nat Med 2003, 9:702-712
23. Bonnarens F, Einhorn TA: Production of a standard closed fracture in laboratory animal bone. J Orthop Res 1984, 2:97-101
24. Kokubu T, Hak DJ, Hazelwood SJ, Reddi AH: Development of an atrophic nonunion model and comparison to a closed healing fracture in rat femur. J Orthop Res 2003, 21:503-510
25. Michalet X, Pinaud FF, Bentolila LA, Tsay JM, Doose S, Li JJ, Sundaresan G, Wu AM, Gambhir SS, Weiss S: Quantum dots for live cells, in vivo imaging, and diagnostics. Science 2005, 307:538-544

26. Akerman ME, Chan WC, Laakkonen P, Bhatia SN, Ruoslahti E: Nanocrystal targeting in vivo. Proc Natl Acad Sci USA States of America 2002, 99:12617-12621
27. Linden M, Sirsjo A, Lindbom L, Nilsson G, Gidlof A: Laser-Doppler perfusion imaging of microvascular blood flow in rabbit tenuissimus muscle. Am J Physiol 1995, 269:H1496-1500
28. Wardell K, Jakobsson A, Nilsson GE: Laser Doppler perfusion imaging by dynamic light scattering. IEEE T Bio-Med Eng 1993, 40:309-316
29. Kendall RL, Thomas KA: Inhibition of vascular endothelial cell growth factor activity by an endogenously encoded soluble receptor. Proc Natl Acad Sci U S A 1993, 90:10705-10709
30. Allen HL, Wase A, Bear WT: Indomethacin and aspirin: effect of nonsteroidal anti-inflammatory agents on the rate of fracture repair in the rat. Acta Orthop Scand 1980, 51:595-600
31. Hak DJ, Makino T, Niikura T, Hazelwood SJ, Curtiss S, Reddi AH: Recombinant human BMP-7 effectively prevents non-union in both young and old rats. J Orthop Res 2006, 24:11-20
32. Turner CH, Burr DB: Basic biomechanical measurements of bone: a tutorial. Bone 1993, 14:595-608
33. Peng Z, Tuukkanen J, Zhang H, Jamsa T, Vaananen HK: The mechanical strength of bone in different rat models of experimental osteoporosis. Bone 1994, 15:523-532
34. Makino T, Hak DJ, Hazelwood SJ, Curtiss S, Reddi AH: Prevention of atrophic nonunion development by recombinant human bone morphogenetic protein-7. J Orthop Res 2005, 23:632-638
35. Eghbali-Fatourechi G, Khosla S: Purification and Caracteruzation of Circulating Osteoblast Lineage Cells: Expression of Type1 Collagen mRNA Is a Key Difference between these and Adherent Bone Marrow Stromal Cells. J Bone Miner Res 2005, 20:S12
36. Majka M, Janowska-Wieczorek A, Ratajczak J, Ehrenman K, Pietrzkowski Z, Kowalska MA, Gewirtz AM, Emerson SG, Ratajczak MZ: Numerous growth factors, cytokines, and chemokines are secreted by human CD34(+) cells, myeloblasts, erythroblasts, and megakaryoblasts and regulate normal hematopoiesis in an autocrine/paracrine manner. Blood 2001, 97:3075-3085
37. Janowska-Wieczorek A, Majka M, Ratajczak J, Ratajczak MZ: Autocrine/paracrine mechanisms in human hematopoiesis. Stem Cells 2001, 19:99-107
38. Goodell MA, Rosenzweig M, Kim H, Marks DF, DeMaria M, Paradis G, Grupp SA, Sieff CA, Mulligan RC, Johnson RP: Dye efflux studies suggest that hematopoietic

stem cells expressing low or undetectable levels of CD34 antigen exist in multiple species. Nat Med 1997, 3:1337-1345

39. Dominici M, Pritchard C, Garlits JE, Hofmann TJ, Persons DA, Horwitz EM: Hematopoietic cells and osteoblasts are derived from a common marrow progenitor after bone marrow transplantation. Proc Natl Acad Sci USA 2004, 101:11761-11766
40. Olmsted-Davis EA, Gugala Z, Camargo F, Gannon FH, Jackson K, Kienstra KA, Shine HD, Lindsey RW, Hirschi KK, Goodell MA, Brenner MK, Davis AR: Primitive adult hematopoietic stem cells can function as osteoblast precursors. Proc Natl Acad Sci USA 2003, 100:15877-15882
41. Badorff C, Brandes RP, Popp R, Rupp S, Urbich C, Aicher A, Fleming I, Busse R, Zeiher AM, Dimmeler S: Transdifferentiation of blood-derived human adult endothelial progenitor cells into functionally active cardiomyocytes. Circulation 2003, 107:1024-1032
42. Yeh ET, Zhang S, Wu HD, Korbling M, Willerson JT, Estrov Z: Transdifferentiation of human peripheral blood CD34+-enriched cell population into cardiomyocytes, endothelial cells, and smooth muscle cells in vivo. Circulation 2003, 108:2070-2073
43. Zhang S, Wang D, Estrov Z, Raj S, Willerson JT, Yeh ET: Both cell fusion and transdifferentiation account for the transformation of human peripheral blood CD34-positive cells into cardiomyocytes in vivo. Circulation 2004, 110:3803-3807
44. Iwasaki H, Kawamoto A, Ishikawa M, Oyamada A, Nakamori S, Nishimura H, Sadamoto K, Horii M, Matsumoto T, Murasawa S, Shibata T, Suehiro S, Asahara T: Dose-dependent contribution of CD34-positive cell transplantation to concurrent vasculogenesis and cardiomyogenesis for functional regenerative recovery after myocardial infarction. Circulation 2006, 113:1311-1325
45. Ratajczak MZ, Kucia M, Reca R, Majka M, Janowska-Wieczorek A, Ratajczak J: Stem cell plasticity revisited: CXCR4-positive cells expressing mRNA for early muscle, liver and neural cells 'hide out' in the bone marrow. Leukemia 2004, 18:29-40
46. Kucia M, Dawn B, Hunt G, Guo Y, Wysoczynski M, Majka M, Ratajczak J, Rezzoug F, Ildstad ST, Bolli R, Ratajczak MZ: Cells expressing early cardiac markers reside in the bone marrow and are mobilized into the peripheral blood after myocardial infarction. Circ Res 2004, 95:1191-1199
47. Eghbali-Fatourechi GZ, Lamsam J, Fraser D, Nagel D, Riggs BL, Khosla S: Circulating osteoblast-lineage cells in humans. N Engl J Med 2005, 352:1959-1966
48. Taichman RS: Blood and bone: two tissues whose fates are intertwined to create the hematopoietic stem-cell niche. Blood 2005, 105:2631-2639

49. Zhu J, Emerson SG: A new bone to pick: osteoblasts and the haematopoietic stem-cell niche. Bioessays 2004, 26:595-599

50. Zhang J, Niu C, Ye L, Huang H, He X, Tong WG, Ross J, Haug J, Johnson T, Feng JQ, Harris S, Wiedemann LM, Mishina Y, Li L: Identification of the haematopoietic stem cell niche and control of the niche size.[see comment]. Nature 2003, 425:836-841

51. Calvi LM, Adams GB, Weibrecht KW, Weber JM, Olson DP, Knight MC, Martin RP, Schipani E, Divieti P, Bringhurst FR, Milner LA, Kronenberg HM, Scadden DT: Osteoblastic cells regulate the haematopoietic stem cell niche.[see comment]. Nature 2003, 425:841-846

52. Ponomaryov T, Peled A, Petit I, Taichman RS, Habler L, Sandbank J, Arenzana-Seisdedos F, Magerus A, Caruz A, Fujii N, Nagler A, Lahav M, Szyper-Kravitz M, Zipori D, Lapidot T: Induction of the chemokine stromal-derived factor-1 following DNA damage improves human stem cell function. J Clin Invest 2000, 106:1331-1339

53. Quarto R, Mastrogiacomo M, Cancedda R, Kutepov SM, Mukhachev V, Lavroukov A, Kon E, Marcacci M: Repair of large bone defects with the use of autologous bone marrow stromal cells. N Engl J Med 2001, 344:385-386

54. Horwitz EM, Prockop DJ, Fitzpatrick LA, Koo WW, Gordon PL, Neel M, Sussman M, Orchard P, Marx JC, Pyeritz RE, Brenner MK: Transplantability and therapeutic effects of bone marrow-derived mesenchymal cells in children with osteogenesis imperfecta.[see comment]. Nat Med 1999, 5:309-313

55. Petite H, Viateau V, Bensaid W, Meunier A, de Pollak C, Bourguignon M, Oudina K, Sedel L, Guillemin G: Tissue-engineered bone regeneration.[see comment]. Nat Biotechnol 2000, 18:959-963

56. Wakitani S, Imoto K, Yamamoto T, Saito M, Murata N, Yoneda M: Human autologous culture expanded bone marrow mesenchymal cell transplantation for repair of cartilage defects in osteoarthritic knees. Osteoarthr Cartilage 2002, 10:199-206

57. Brugger W, Heimfeld S, Berenson RJ, Mertelsmann R, Kanz L: Reconstitution of hematopoiesis after high-dose chemotherapy by autologous progenitor cells generated ex vivo.[see comment][retraction in Kanz L, Brugger W. N Engl J Med. 2001 Jul 5;345(1):64; PMID: 11439953]. N Engl J Med 1995, 333:283-287

58. Kessinger A, Armitage JO: The evolving role of autologous peripheral stem cell transplantation following high-dose therapy for malignancies. Blood 1991, 77:211-213

Figure legends

Figure 1

Mobilization of mouse Sca1+Lin- cells by fracture stress

(A) Percentage of peripheral blood Sca1+ Lin- cells to Lin- MNCs shows an increase with the peak at day 1 post-fracture. Black line represents isotype control (negative control) and blue line indicates sample data. X axis shows fluorescent intensity of cells, and Y axis demonstrates the number of cells.

(B) Number of Sca1+Lin- cells significantly peaked at day 1 post-fracture, then gradually decreased.

Figure 2

Phenotypic characterization of human peripheral blood mononuclear cells (MNCs) and CD34+ cells by fluorescence-activated cell sorting (FACS) and RT-PCR analysis.

(A) FACS analysis to evaluate positivity for CD34 in MNCs (left panel) and CD34+ cells (right panel). Numbers are percentages of the cells positive for CD34.

(B) FACS analysis to characterize CD34+ cells by positivity for various cell surface markers. Human CD34+ cells were positive for CD133, c-Kit, CD45, CD31 and CD105, and negative for VE-cad, KDR and Tie2. Numbers are percentages of double-positive cells for CD34 (Y axis) and each antibody (X axis).

(C, D) RT-PCR analysis for human-specific genes of endothelial (C) and osteoblastic (D) lineages was performed in freshly isolated CD34+ cells and MNCs. The analysis of CD34+ cells revealed weak expression of hCD31 and human osteocalcin (hOC) but not of the other endothelial marker (hVE-cad) and bone-related marker (hCol1A1). Cultured human umbilical vein endothelial cells (HUVECs) and osteoblasts (OBs) were used for positive control for human-specific endothelial and bone-related

genes.

(E) RT-PCR analysis at the single cell level of the CD34+ cells. Four out of 20 CD34+ cells expressed both CD34 and hOC.

Figure 3

Recruitment of fluorescent-labeled CD34+ cells into fracture site

(A-C) Histochemical staining for isolectin B4 (green), a rat-specific endothelial cell (EC) marker, using tissue samples of fracture sites obtained from rats receiving Qtracker-labeled human cells (red) 1 week post-fracture in the granulation area shown as *zone a* in Figure 3M. More efficient recruitment of human cells with neovasculature-like structure was accompanied with enhancement of neovascularization by recipient rat cells in animals treated with CD34+ cells (A) compared with those receiving MNCs (B) or PBS alone (C) (x 100).

(D-F) Double fluorescent immunostaining for human leukocyte antigen (HLA)-ABC (red) and smooth muscle actin (green) using the tissue sample of granulation area. The massive recruitment of the human cells in the granulation area with relatively rare incorporation along the inner layer of SMA–positive smooth muscle cells were observed in CD34+ group. The human cells lining along the inner layer were morphologically compatible with endothelial cells (D). In contrast, less recruitment of human cells in the granulation area and no human cells along the inner layer of arterioles were observed in animals receiving MNCs (E). Human cells were not found in PBS group (F) (x 200).

(G-I) Persuit of Qtracker-labeled human cells 1 week post-fracture in newly bone formed area shown as *zone b* in Figure 3M. Human cell (red) recruitment into the newly formed bone area (surrounded by broken lines) was more abundantly observed in animals treated with CD34+ cells (G) compared with those receiving MNCs (H) or PBS alone (I) (x 100).

(J-L) Fluorescent immunohistochemistry for HLA-ABC demonstrated massive recruitment of human cells (red: arrows) in CD34+ group (J). In contrast, less recruitment of the HLA-ABC-positive cells was observed in animals receiving MNCs (K) and no human cells in PBS group (L) (x 200).

(M) Representative photomicrograph of immunostaining for isolectin B4 (brown) and toluidine blue counter staining for anatomical indication of following areas: *zone a*, granulation zone; *zone b*, newly formed bone zone; cb, cortical bone; ca, cartilage; wb, woven bone) (x 40)

(O) The number of HLA-ABC-positive cells observed in *zone a* was significantly greater in CD34+ group compared with other groups. **, $P<0.01$.

(P) The number of HLA-ABC-positive cells in *zone b* was significantly greater in CD34+ group compared with other groups. *, $P<0.05$; **, $P<0.01$.

Blue fluorescence indicates DAPI for nuclear staining. Scale bars in A-C and G-F: 100μm; scale bars in D-F and J-L: 50μm.

Figure 4

Human CD34+ cell-derived vasculogenesis and osteogenesis

Immunohistochemical staining and RT-PCR for human-specific EC or OB markers was performed using tissue samples harvested at week 2.

(A-D) Differentiated human ECs were identified in *zone a* as hCD31-positive cells (red) in animals receiving CD34+ cells (A: x 200, D: x 400) compared with MNC (B) or PBS group (C) (x 200).

(E) RT-PCR analysis of tissue RNA isolated from the peri-fracture site demonstrated the expression of human specific EC markers (hCD31, hVE-cad) in animals treated with CD34+ cells, but not in control animals. Cultured HUVECs were used for positive control, and no RNAs were for negative control.

(F-I) Differentiated human OBs were identified in *zone b* as hOC-positive cells (red) in animals receiving

CD34+ cells (F: x 200, I: x 400) compared with MNC (G) or PBS group (H) (x 200).

(J) RT-PCR analysis of RNA isolated from the peri-fracture site demonstrates the expression of human specific bone-related markers (hOC, hCol1A1) in animals treated with CD34+ cells, but not in control animals. Cultured hOBs were used for positive control.

Blue fluorescence represents DAPI. Broken lines; newly formed bone suface, Scale bars in A-C and F-H, 50μm; scale bars in D and I: 20μm

Figure 5

Enhanced intrinsic vascularization and osteogenesis by recipient's cells and serial improvement of blood flow and enhancement of callus formation following CD34+ cell transplantation

(A) Rat-specific vascular staining with isolectin B4 (brown) at week 2 demonstrated enhanced neovascularization in *zone a* in animals treated with CD34+ cells compared with those receiving MNCs or PBS alone (x200). Intrinsic angiogenesis assessed by capillary density at week 2 was significantly enhanced following CD34+ cell transplantation compared with other treatments. **, $P<0.01$.

(B) Representative laser Doppler perfusion imaging (LDPI) at week 0 (1 hour after fracture) and week 2 in each group. In these digital color-coded images, maximum perfusion values are indicated in white, medium values in green to yellow, and lowest values in dark blue. The skin blood flow within fracture site (red square) and intact contralateral site (black square) were evaluated as mean flux, and ratio of the mean flux in the fractured site with that in the contralateral site (mean flux ratio) was calculated. Severe reduction of the blood flow was similarly observed 1 hour after fracture with the periosteum cauterized in all groups, whereas the mean flux ratio at week 2 was significantly greater in animals treated with CD34+ cells compared with those receiving MNCs or PBS alone. *, $P<0.05$.

(C) Rat-specific OC staining (brown) to detect intrinsic OBs at week 2 revealed augmentation of

osteogenesis in *zone b* in animals treated with CD34+ cells compared with those receiving MNCs or PBS alone (x200). Intrinsic osteogenesis assessed by the OB density at week 2 was significantly enhanced following CD34+ cell transplantation compared with other groups. **, P<0.01. Scale bar: 50μm

(D) Relative callus area assessed by radiograph at week 2 was significantly larger in CD34+ group compared with other groups. *, P<0.05.

Figure 6

Inhibition of intrinsic angiogenesis and osteogenesis by antiangiogenic agent in animals receiving CD34+ cell transplantation

(A) RT-PCR revealed that fractured tissue sample contained higher amount of angiogenic factors (hVEGF, hFGF2 and hHGF) in human CD34+ group compared to MNC group.

(B) Rat-specific vascular staining with isolectin B4 (brown) at week 2 demonstrated reduced neovascularization in *zone a* in animals treated with CD34+ cells and sFlt1 compared with those receiving CD34+ cells and PBS (x200). Intrinsic angiogenesis assessed by capillary density at week 2 is significantly reduced following sFlt1 treatment compared to PBS. *, P<0.05.

(C) Representative LDPI at weeks 0 and 2 in each group (red square, fracture site; black square, intact contralateral site). Mean flux ratio at week 2 was significantly less in animals treated with sFlt1 compared to rats receiving PBS. *, P<0.05.

(D) Representative rat-specific OC staining (brown) to detect intrinsic OBs at week 2 in *zone b* in animals treated with CD34+ cells and sFlt1and those receiving CD34+ cells and PBS (x200). Intrinsic osteogenesis assessed by the OB density at week 2 was significantly inhibited following sFlt1 treatment compared to PBS. *, P<0.05.

(E) Relative callus area assessed by radiograph at week 2 was significantly smaller in sFlt1 treated group

compared to PBS group. *, P<0.05.

Figure 7

Radiographical, histological and biomechanical evidence of fracture healing following CD34+ cell transplantation

(A) Fracture healing was serially assessed by radiographs. By week 8, fracture was healed with bridging callus in all animals receiving CD34+ cells, but in no rats treated with MNCs or PBS alone.

(B) Serial assessment of fracture healing by histological examination with toluidine blue staining. Histological evaluation demonstrated the enhanced endochondral ossification consisting of numerous chondrocytes and newly formed trabecular bone at week 2, bridging callus formation at week 4 and complete union at week 8 in animals receiving CD34+ cell transplantation. Although a thick callus formation at week 2 was observed, the healing process had stopped by week 4 and finally the callus was absorbed at week 8 in animals receiving MNCs or PBS.

(C) The degree of fracture healing was assessed by Allen's classification. The degree of fracture healing at weeks 4 and 8 was significantly higher following CD34+ cell transplantation compared with other treatments. *, P<0.05; **, P<0.01.

(D) Functional recovery following fracture is assessed by biomechanical three-point bending test at week 8. The percentage of all parameters (%ultimate stress, %extrinsic stiffness, %failure energy) showing the ratio of each value in fractured side with contralateral side in animals receiving CD34+ cells was significantly superior to those in animals receiving MNCs or PBS. *, P<0.05.

Figure 1

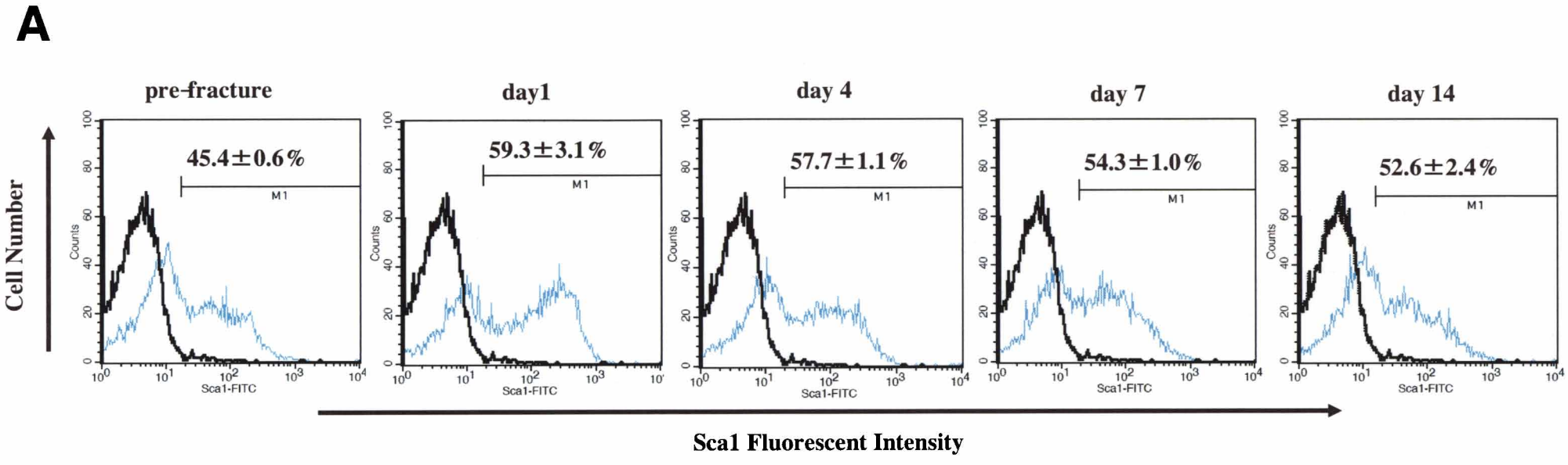
A
pre-fracture
day1
day 4
day 7
day 14
45.4±0.6%
59.3±3.1%
57.7±1.1%
54.3±1.0%
52.6±2.4%
M1
Counts
Sca1-FITC
Cell Number
Sca1 Fluorescent Intensity

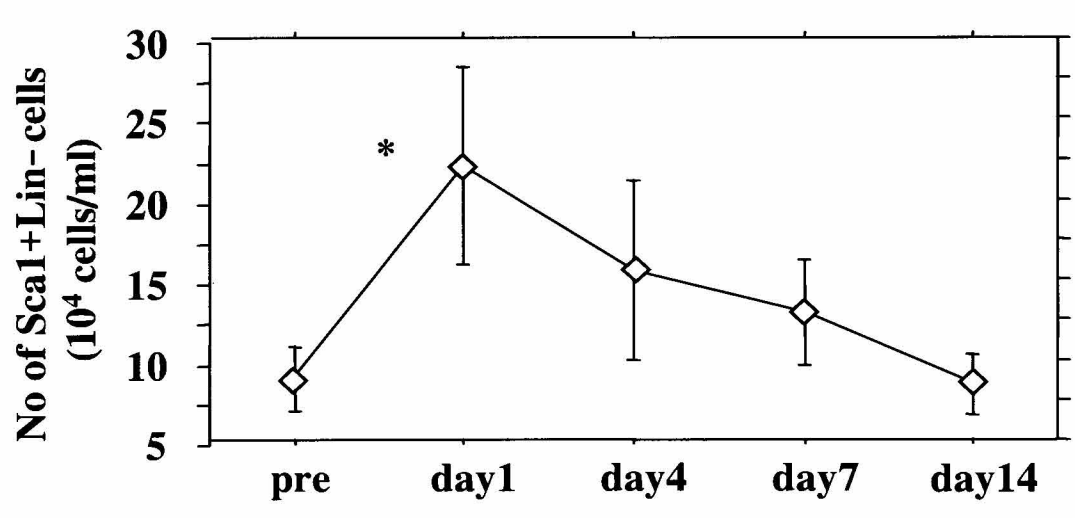
B
No of Sca1+Lin- cells
(10⁴ cells/ml)
30
25
20
15
10
5
*
pre
day1
day4
day7
day14

Figure 2

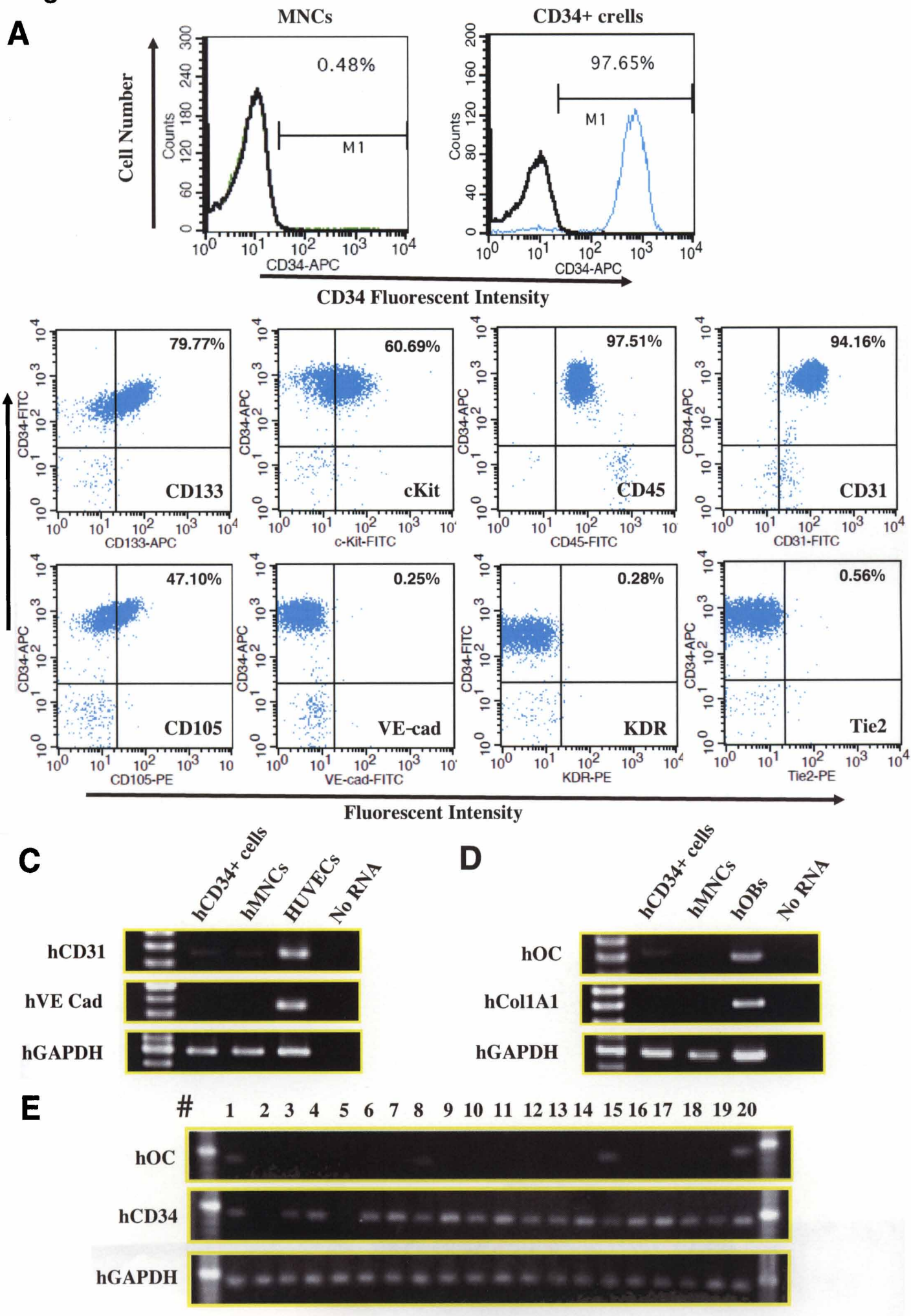
A
MNCs
CD34+ crells
Cell Number
Counts
0.48%
97.65%
M1
CD34-APC
CD34 Fluorescent Intensity
B
CD34 Fluorescent Intensity
79.77%
CD133
CD133-APC
CD34-FITC
60.69%
cKit
c-Kit-FITC
CD34-APC
97.51%
CD45
CD45-FITC
94.16%
CD31
CD31-FITC
47.10%
CD105
CD105-PE
0.25%
VE-cad
VE-cad-FITC
0.28%
KDR
KDR-PE
0.56%
Tie2
Tie2-PE
Fluorescent Intensity
C
hCD34+ cells
hMNCs
HUVECs
No RNA
hCD31
hVE Cad
hGAPDH
D
hCD34+ cells
hMNCs
hOBs
No RNA
hOC
hCol1A1
hGAPDH
E
1 2 3 4 5 6 7 8 9 10 11 12 13 14 15 16 17 18 19 20
hOC
hCD34
hGAPDH

Figure 3

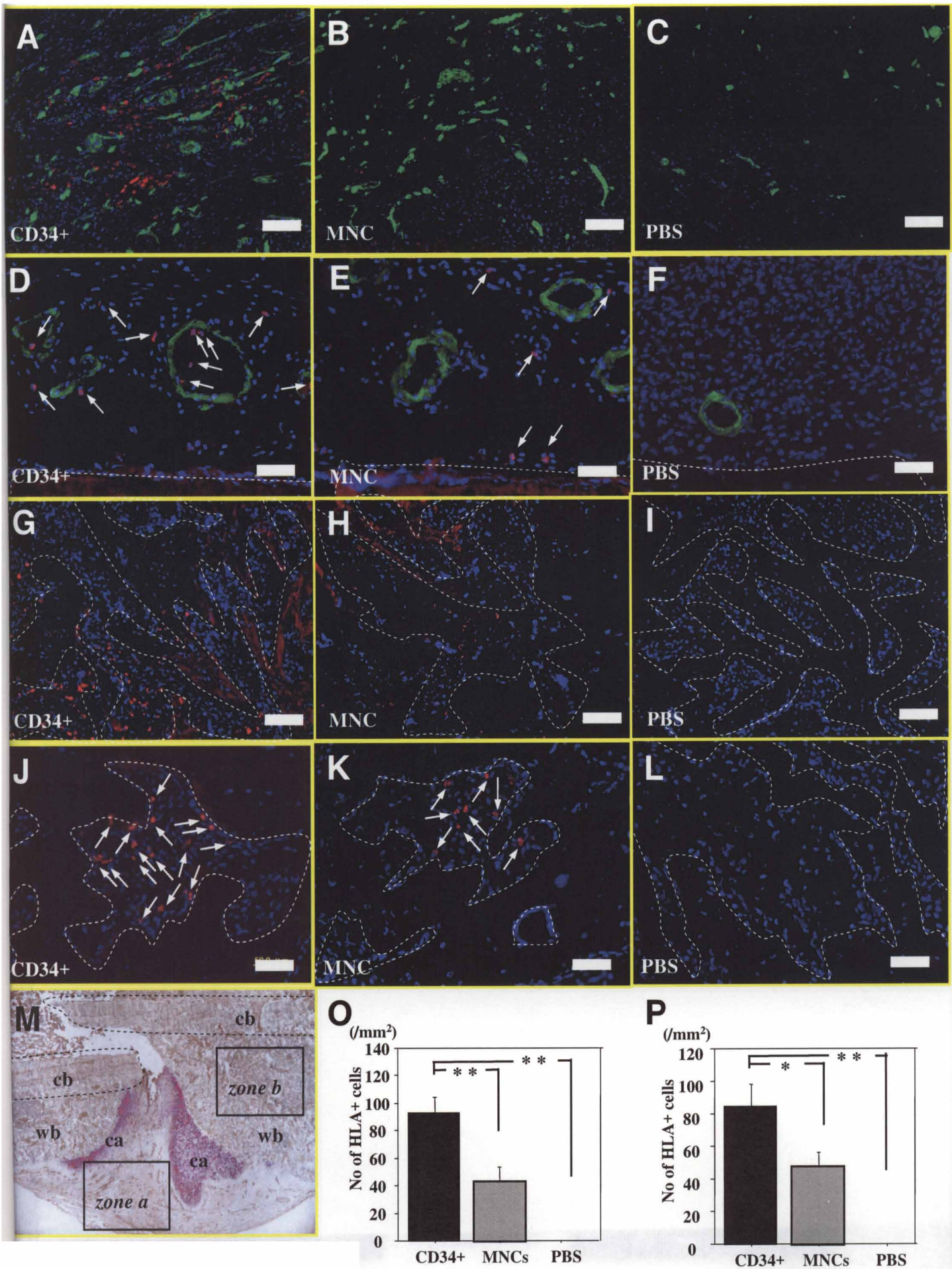
A
CD34+
B
MNC
C
PBS
D
CD34+
E
MNC
F
PBS
G
CD34+
H
MNC
I
PBS
J
CD34+
K
MNC
L
PBS
M
cb
cb
zone b
wb
ca
wb
ca
zone a
O
(/mm²)
No of HLA+ cells
140
120
100
80
60
40
20
0
* *
* *
CD34+
MNCs
PBS
P
(/mm²)
No of HLA+ cells
120
100
80
60
40
20
0
*
* *
CD34+
MNCs
PBS

Figure 4

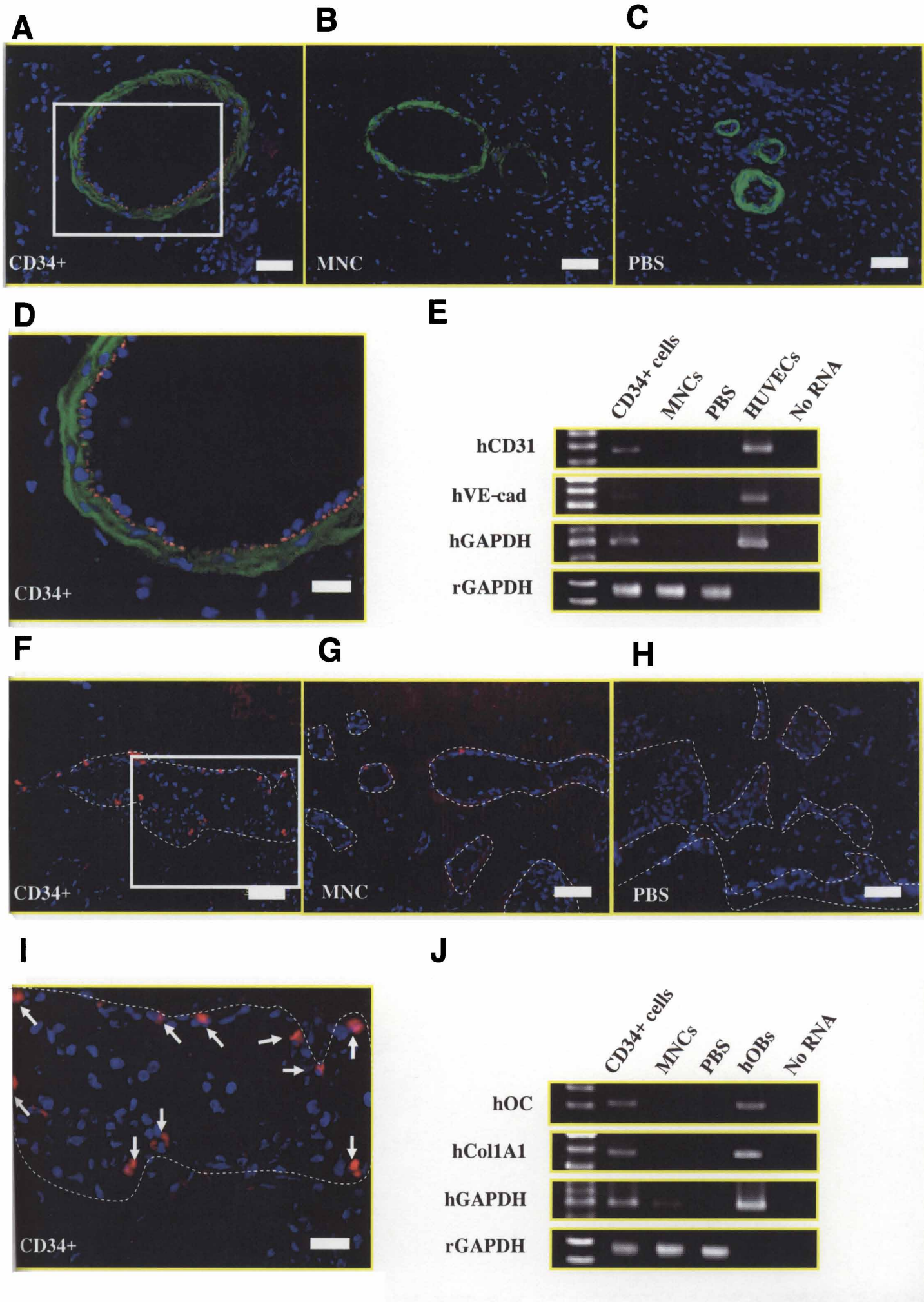
A
B
C
CD34+
MNC
PBS
D
CD34+
E
CD34+ cells
MNCs
PBS
HUVECs
No RNA
hCD31
hVE-cad
hGAPDH
rGAPDH
F
G
H
CD34+
MNC
PBS
I
CD34+
J
CD34+ cells
MNCs
PBS
hOBs
No RNA
hOC
hCol1A1
hGAPDH
rGAPDH

Figure 5

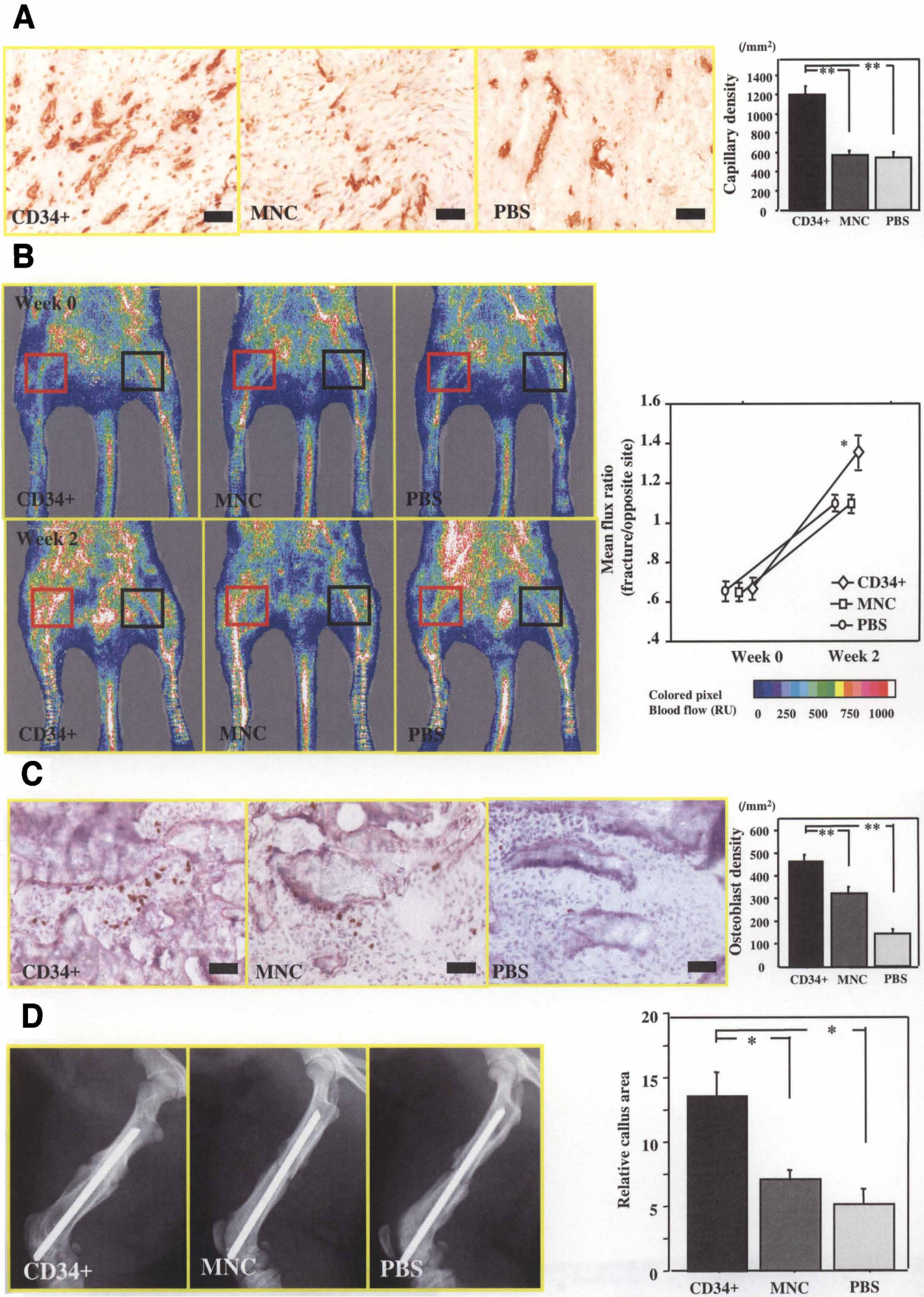
A
CD34+
MNC
PBS
(/mm²)
Capillary density
1400
1200
1000
800
600
400
200
0
**
**
CD34+
MNC
PBS
B
Week 0
Week 2
CD34+
MNC
PBS
Mean flux ratio
(fracture/opposite site)
1.6
1.4
1.2
1
.8
.6
.4
*
CD34+
MNC
PBS
Week 0
Week 2
Colored pixel
Blood flow (RU)
0
250
500
750
1000
C
CD34+
MNC
PBS
(/mm²)
Osteoblast density
600
500
400
300
200
100
0
**
**
CD34+
MNC
PBS
D
CD34+
MNC
PBS
Relative callus area
20
15
10
5
0
*
*
CD34+
MNC
PBS

Figure 6

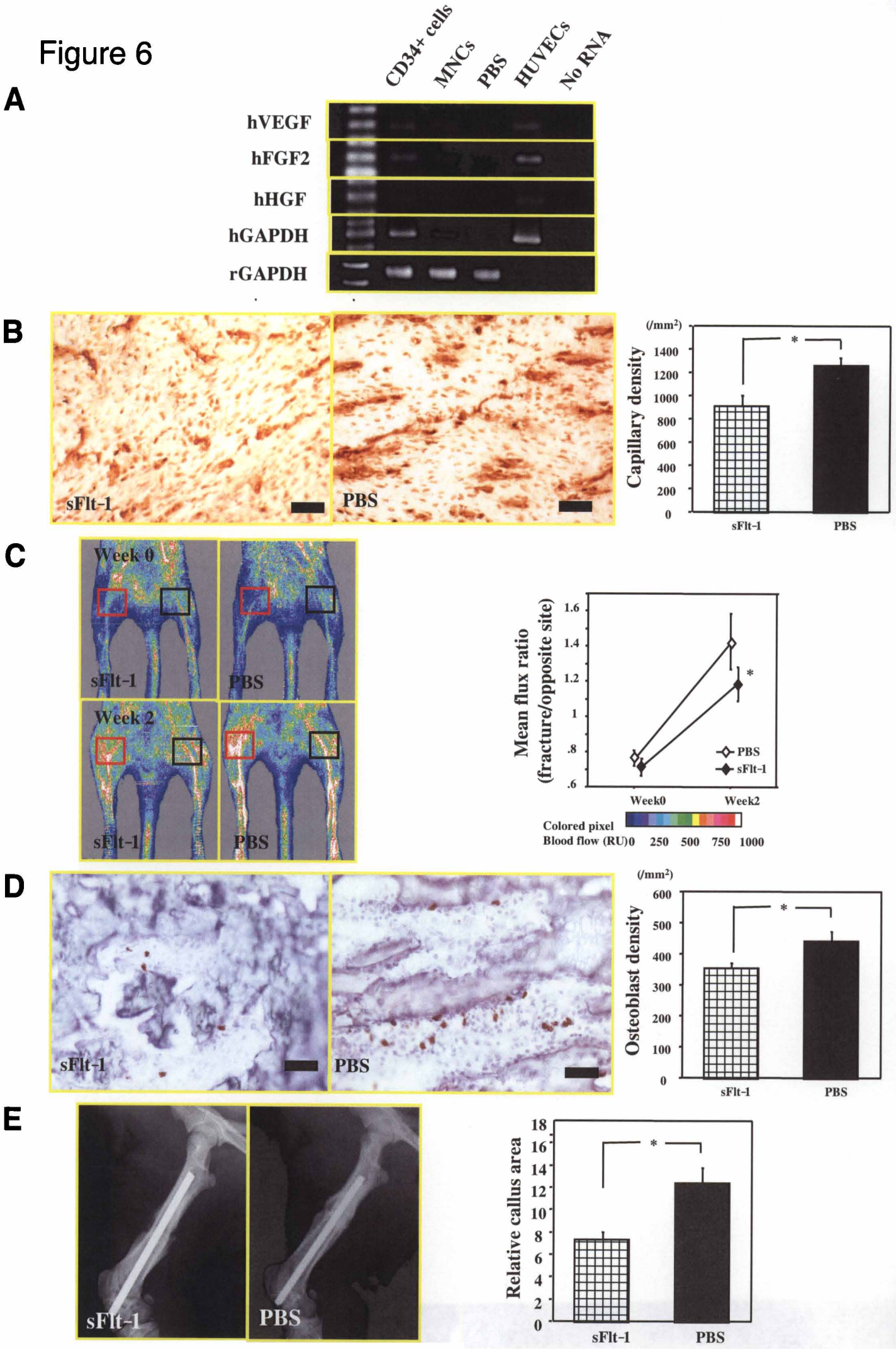
A
CD34+ cells
MNCs
PBS
HUVECs
No RNA
hVEGF
hFGF2
hHGF
hGAPDH
rGAPDH
B
sFlt-1
PBS
(/mm²)
Capillary density
1400
1200
1000
800
600
400
200
0
*
sFlt-1
PBS
C
Week 0
Week 2
sFlt-1
PBS
sFlt-1
PBS
Mean flux ratio
(fracture/opposite site)
1.6
1.4
1.2
1
.8
.6
*
PBS
sFlt-1
Week0
Week2
Colored pixel
Blood flow (RU) 0 250 500 750 1000
D
sFlt-1
PBS
(/mm²)
Osteoblast density
600
500
400
300
200
100
0
*
sFlt-1
PBS
E
sFlt-1
PBS
Relative callus area
18
16
14
12
10
8
6
4
2
0
*
sFlt-1
PBS

Figure 7

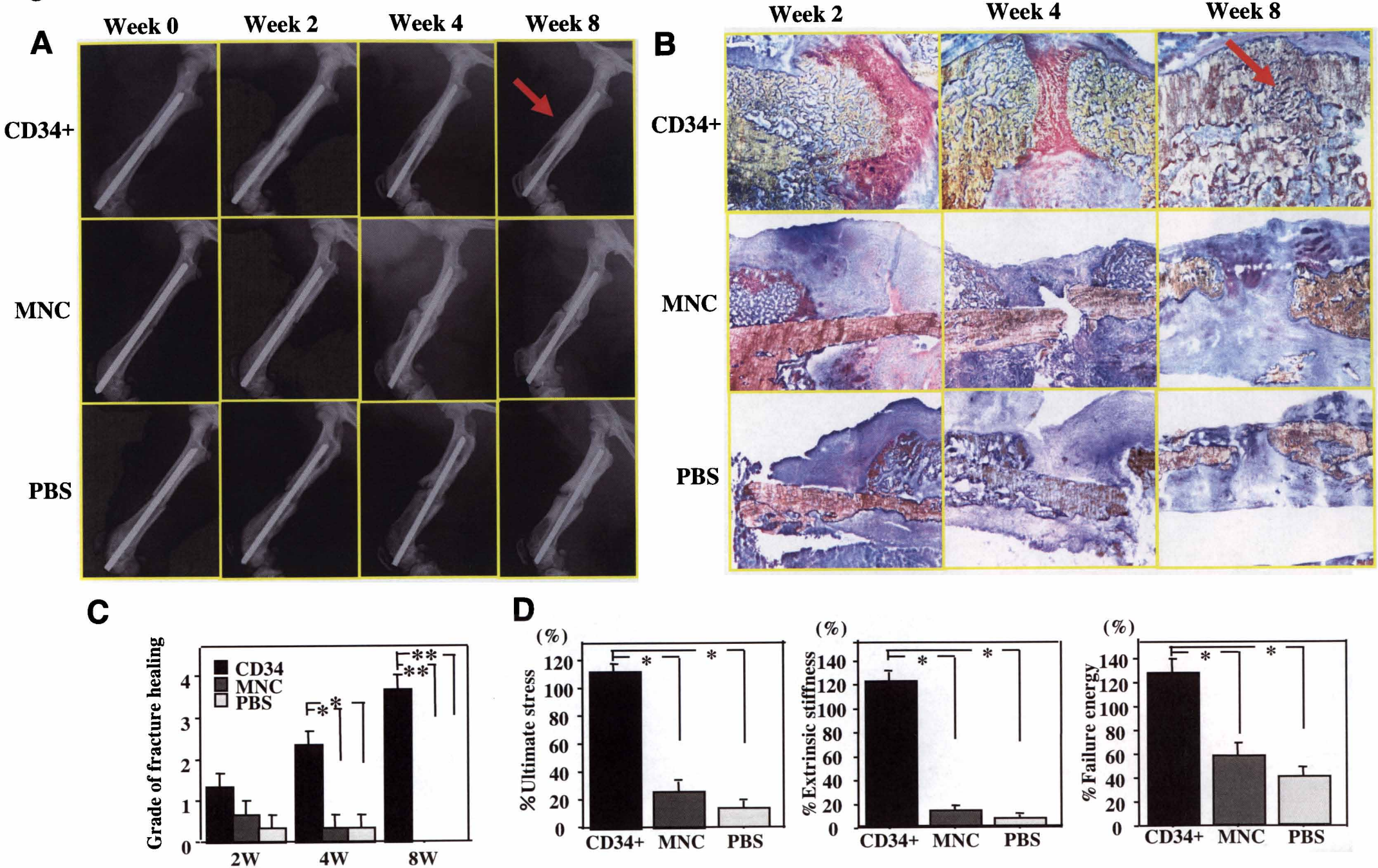
A
Week 0
Week 2
Week 4
Week 8
CD34+
MNC
PBS
B
Week 2
Week 4
Week 8
CD34+
MNC
PBS
C
Grade of fracture healing
CD34
MNC
PBS
2W
4W
8W
D
(%)
% Ultimate stress
% Extrinsic stiffness
% Failure energy
CD34+
MNC
PBS